Precoded transmission in TDD mode for LTE-A Uplink

Author:
William Szacowny

Supervisors:
Gilberto Berardinelli
Troels B. Sorensen

AALBORG UNIVERSITY

Department of Electronic Systems
Fredriks Bajers Vej 7

Title:

Precoded transmission in TDD mode for LTE-A Uplink

Project period:

February – June 2010

Project group:

gr 1093

Participant:

William Szacowny

Supervisors:

Gilberto Berardinelli
Troels B. Sorensen

Copies: 3

Date:

June 3^{rd}, 2010

Abstract:

Long Term Evolution – Advanced (LTE-A) mobile communication systems are currently being standardized. Since performance requirements of the air interface are very high, LTE-A provides several new features compared to LTE.
Given the high performance requirements of LTE-A, performances of precoded transmission in TDD, and more specifically in open-loop transmission, are going to be evaluated. Different precoding solutions are considered in order to obtain relevant comparisons and to quantify the amount of gain provided by each precoding technique.
Techniques as *Blind Transmission*, *Precoded Pilots* and *Phase Based Precoding* are going be evaluated. The influence of different parameters is also quantified to discuss their impact on performance of precoded transmissions in TDD.

Contents

List of Figures

List of Acronyms

3GPP	3rd Generation Partnership Project
LTE	Long Term Evolution
GSM	Global System for Mobile communications
UMTS	Universal Mobile Telecommunications System
ITU	International Telecommunication Union
IMT	International Mobile Telecommunications
SU-MIMO	Single User Multiple Input Multiple Output
MU-MIMO	Multi User Multiple Input Multiple Output
HSPA	High Speed Packet Access
CDMA	Code Division Multiple Access
EV-DO	Evolution-Data Optimized
WiMax	Worldwide Interoperability for Microwave Access
UE	User Equipment
TDD	Time Duplex Division
FDD	Frequency Duplex Division
MIMO	Multiple Input Multiple Output

SM	Spatial Multiplexing
SFBC	Space-Frequency Block Coding
FSTD	Frequency-Shift Time Diversity
CSI	Channel State Information
CoMP	Coordinated Multipoint Transmission
QAM	Quadrature Amplitude Modulation
QPSK	Quadrature Phase-Shift Keying
OFDMA	Orthogonal Frequency Division Multiple Access
OFDM	Orthogonal Frequency Division Multiplexing
SC-FDMA	Single-Carrier Frequency Division Multiple Access
SCFDM	Single-Carrier Frequency Division Multiplexing
ISI	Inter-Symbol Interference
CP	Cyclic Prefix
PAPR	Peak-to-Average Power Ratio
IFFT	Inverse Fast Fourier Transform
SVD	Singular Value Decomposition
DFT	Discrete Fourier Transform
FFT	Fast Fourier Transform
AWGN	Additive White Gaussian Noise
ANSI	American National Standards Institute
GP	Guard Period
UpPTS	Uplink Pilot Time Slot
DwPTS	Downlink Pilot Time Slot

PSS	Primary Synchronisation Signal
SSS	Secondary Synchronization Signal
UL	Uplink
DL	Downlink
MMSE	Minimum Mean Square Error
WF	Wiener Filter
RF	Radio Frequency
SIMO	Single Input Multiple Output
MCS	Modulation and Coding Scheme
BLER	Block Error Ratio
CRC	Cyclic Redundancy Check
CDF	Cumulative Distribution Function
PDF	Probability Density Function
CCDF	Complementary Cumulative Distribution Function
PDP	Power Delay Profile
TU20	Typical Urban channel with a PDP of 20 paths
SNR	Signal-to-Noise Ratio

Chapter 1

Introduction

1.1 Introduction

1.1.1 General Background

As multimedia communications become increasingly popular, mobile communications are expected to reliably support high data rate transmissions. In this way, many improvements have been made during these past years through several generations of mobile communication systems.

Recently, the 3rd Generation Partnership Project (3GPP) has reached a mature state in the specification of Long Term Evolution (LTE) standardization [1] . This new standard, also known as the fourth generation of mobile network systems, allows the use of a couple of new technologies which give the opportunity to have high capabilities compared to previous generations. Since the end of 2009, LTE mobile communication systems started to be deployed as the next generation of mobile communication. It is considered as a natural evolution of previous generations known as Global System for Mobile communications (GSM) and Universal Mobile Telecommunications System (UMTS).

In parallel, the International Telecommunication Union (ITU) has worked to define new standard requirements to identify new mobile systems with high capabilities. As a result, International Mobile Telecommunications (IMT)-Advanced was released this past year. Before this specification, systems were defined through the IMT-2000, but IMT-Advanced has

more strict requirements, essentially in data rate in order to support advanced services and applications. Throughout the year 2009, 3GPP has worked with the purpose of identifying which LTE improvements are required to respect the IMT-Advanced specification. In October 2009, the 3GPP Partners made a formal submission to the ITU by proposing LTE Release 10 and beyond (also called LTE- Advanced) [9] . They considered that this new release should be evaluated as a candidate for IMT-Advanced.

To achieve this diverse set of objectives imposed by the ITU, LTE-Advanced adopts various MIMO technologies including transmit diversity, spatial multiplexing, Single User (SU)-MIMO, MultiUser (MU)-MIMO, closed-loop and opened-loop precoding, and dedicated beamforming [3] .

IMT-Advanced requirements also depend of transmission scheme, meaning they differ between uplink and downlink channels. If we consider a SU-MIMO scheme, it is specified for the configuration with two or four transmit antennas in the uplink, and up to eight transmit antennas in the downlink, which supports transmission of multiple spatial layers with up to four layers to a given User Equipment (UE).

1.1.2 Motivations

According to requirements that LTE-Advanced has to respect, this project will be focused on performance of precoded MIMO transmission over the uplink channel. Basically, precoding is aimed to exploit some channel information in order to improve performance of transmission. Since LTE-Advanced supports Time Duplex Division (TDD) and Frequency Duplex Division (FDD) modes, different precoding techniques are evaluated, respectively in open-loop and closed-loop transmissions.

Several known issues are going to be evaluated in an open-loop transmission in order to quantify the gain that each technique can provide on a transmission of single data stream over spatially multiplexed channels. The feasibility of a practical implementation is also going to be evaluated to find a realistic and an efficient precoding scheme.

1.2 Mobile multipath channel

The mobile propagation radio channel is one of the fundamental limitations for mobile communication systems. The trajectory of transmission between a transmitter and a receiver could be severely obstructed due to buildings, mountains and vegetation in an outdoor environment or due to different compositions of walls in an indoor environment. These different obstacles introduce several phenomena which have a direct influence on the channel. In addition, the state of the channel is affected by the movement of the receiver and the obstructive elements. For this reason, the mobile channel could be randomly modelled assuming specific distributions and has a propagation which is split into several beams, this phenomenon is called multipath. The figure 1.1 illustrates some well known phenomena which create multipath in a generic outdoor propagation example.

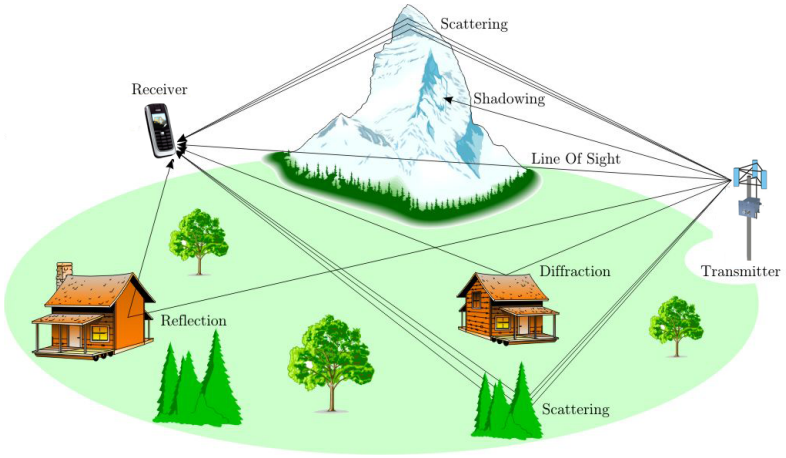

Figure 1.1: Generic Example of a Multipath channel (Outdoor)

The presence of a multiple path propagation between a transmitter and a receiver is a principal cause of unreliability of digital mobile radio systems. In particular, the mobile nature of the receiver, transmitter and other objects in the environment causes the channel characteristics to change continually.

In mobile communication systems, the knowledge of this channel is needed to properly perform detection and estimations tasks in the receiver. If the behaviour of the channel is known, the performance of a system using the channel can be optimised for the particular conditions being experienced at that instant. This optimisation can take the form of change in transmission timing, frequency, power level, modulation type, coding and precoding, as

well as some implementations of MIMO systems.

1.3 MIMO

Multiple input multiple output (MIMO) is one of several forms of smart antenna technology. It has been treated as an emerging technology to meet the demand for higher data rate and better cell coverage even without increasing average transmit power or frequency bandwidth. It has been proved that a MIMO structure successfully constructs multiple spatial layers where multiple data streams are delivered on a given frequency-time resource and linearly increases the channel capacity [23]. So, this technology can achieve transmissions with higher spectral efficiency (more bits per second per hertz of bandwidth) and link reliability or diversity (reduced fading).

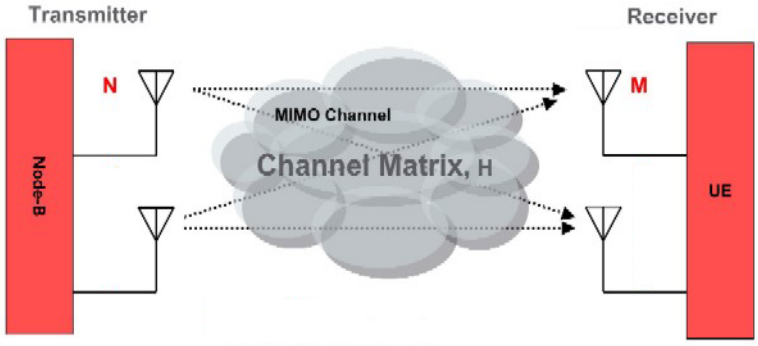

Figure 1.2: Multiple Input Multiple Output scheme

The principle of this technology is defined by using several antennas as transmitters and receivers as the figure 1.2 shows it. The number of transmit antennas is defined by N and the number of receive antennas by M. It is assumed that $N \leqslant M$ has to be verified to have an efficient transmission over multiple parallel channels defined by the matrix H :

$$\mathbf{H} = \begin{pmatrix} h_{11} & h_{12} & \dots & h_{1N} \\ h_{21} & h_{22} & & \vdots \\ \vdots & & \ddots & \vdots \\ h_{M1} & \dots & \dots & h_{MN} \end{pmatrix} \tag{1.1}$$

where h_{ij}, denotes the complex channel gain from the transmit antenna j to the receive antenna i with $i = [1, 2, \ldots, M]$ is the number of the transmit antenna and $i = [1, 2, \ldots, N]$ is the number of the received antenna.

In order to define the transmission scheme, a MIMO system is modelled by :

$$\mathbf{y} = \mathbf{H}\mathbf{x} + \mathbf{n} \tag{1.2}$$

where $\mathbf{x} = [x_1, x_2, \ldots, x_N]^T$ is the $N \times 1$ vector of transmitted symbols, $\mathbf{y}$ is the $M \times 1$ vector of received symbols, $\mathbf{H}$ is the channel matrix defined previously, and $\mathbf{n}$ the M-dimensional additive Gaussian noise vector.

MIMO technologies also introduces in LTE-Advanced (and previously in LTE) several important notions such as spatial multiplexing, transmit diversity, and beamforming. These notions are key components for providing higher peak rate at a better system efficiency, which is essential for supporting future data services and applications over wireless links.

1.3.1 Spatial multiplexing

Spatial multiplexing (SM) is a transmission technique in MIMO wireless communication which transmit independent and separately several encoded data signals (streams), from each of the multiple transmit antennas over several independent (spatial) channels.

As we saw before in the MIMO section 1.3, we consider that the transmitter is equipped with N antennas and the receiver with M antennas. If a linear receiver is used, the maximum spatial multiplexing order is defined as :

$$N_s = \min(M, N) \tag{1.3}$$

where N_s is the number of streams which can be transmitted in parallel.

If we resume characteristics of SM:

- No bandwidth expansion to increase data rates.
- Space–time equalization needed in the receiver.
- Conventionally: Number of Receive Antennas (N) $\geq$ Number of Transmit Antennas (M)

- The data streams can be separated by the equalizer, if fading processes of the spatial channels are (nearly) independent.
- Actual MIMO channel with capacity linearly increasing the number of antennas or more precisely independent spatial channels.

1.3.2 Transmit diversity

Since we consider only the LTE-Advanced uplink channel, it means only a transmission from a UE to an eNodeB is considered (an eNodeB is an enhanced BTS which provides the LTE-Advanced air interface and performs radio resource management for evolved access system). In LTE-Advanced, the UE is able to use up to four antennas but we consider only two transmit antennas is order to simplify the explanation of the principle of transmit diversity.

Transmit diversity is also one of MIMO technologies. The principle of this technique is to send the same information through both antennas. However, data from the second antenna is encoded differently to distinguish it from the first antenna. By receiving these signals, the receiver must be able to recognize that signals come from two different sources and then, a properly decoding of data becomes possible.

In other words, the aim of transmit diversity is exploiting redundancy across frequency or time by generating multiple replicas of the same transmit signals. This redundancy permits to have a certain robustness against undesirable effects of fading, outages, or circuit failures. To achieve this robustness, transmit antenna selection diversity is based on Space-Frequency Block Coding (SFBC) techniques and it is complemented with Frequency-Shift Time Diversity (FSTD) if four transmit antennas are used [13].

The impact of transmit diversity is different according to the scheme of transmission used [17]. There is a significant difference between the closed-loop and the open-loop (sections 2.4 and 3.1, respectively, give a detailed description of these schemes of transmission) transmit antenna selection. In the case of closed-loop transmit antenna selection, the eNodeB selects the antenna to be used for uplink transmission and communicate this selection to the UE using a downlink control message. However, for an open-loop transmit antenna selection, the UE autonomously selects the transmit antenna to be used for transmission without intervention of the eNodeB.

1.3.3 Beamforming

When some waves are combining on the same frequency, they can be manipulated in a way to be combined constructively or destructively. Beamforming technology uses this principle in the spatial and temporal domains. On the receiver side, there are multiple spatial samples of waves, a beamformer can enhance or cancel a wave coming from a certain direction. Similar on the transmitter side, multiple spatial transmitters can transmit waves so that the radiation pattern is coherent or destructive in desired direction. This technique can be applied for every kind of waves.

If we consider MIMO aspect, Beamforming is a signal processing technique with the particularity of using a fading channels to their advantage. In a multipath fading channel, as it is introduced in section 1.2, the non-line-of-sight paths degrade the signal since the receiver would receive multiple copies of a signal with variation in time and strength.

It creates a transmission radiation pattern that is focused in directions where the communication is the most reliable communication as the figure 1.3 shows it. It consists of an array of antennas that together direct different transmission/reception beams toward each user in the system.

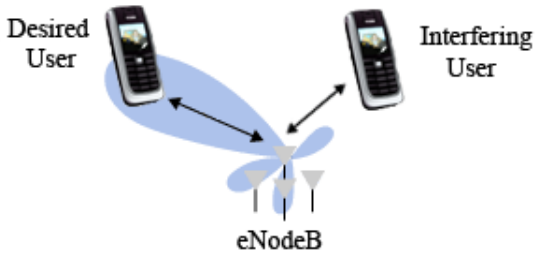

Figure 1.3: Beamforming with a smart antenna

However, to successfully achieve it, it is required a reliable knowledge of the channel. Based on the amount of information known on the channel, the type of beamforming is selected, this technique is called adaptive beamforming. Three different scenarios are possible :

- Full Channel State Information (CSI) : In this case, statistical eigenvector beamforming is a reliable and commonly implemented solution.

- Limited CSI : Techniques such as Grassmannian or interpolation beamforming are typically used.
- No CSI : Blind beamforming techniques are used, in which the channel state information is blindly estimated from the received signal statistics.

To fully use the benefits of the beamforming in a MIMO wireless system, one must learn how the channel state information is going to obtained and have some knowledge of channel characteristics. This will help ensure that the proper beamforming technique is applied.

Moreover, since we considered a MIMO system, beamforming has to support a multi-layer transmission which is not possible with a conventional one. The principle of conventional beamforming can be efficient if a receiver with a single antenna is considered because it consists in an appropriate weighting applied on the identical transmit signal from each of the transmit antennas and then, the received signal power can be maximized.

However, when the receiver has multiple antennas, it is easy to understand that a conventional beamforming cannot simultaneously maximize the signal level for each receive antenna. In order to maximize it, a multi-layer beamforming is needed and obtained by using precoding.

So, we can define precoding as a generalized beamforming which permits to maximize the received signal level by applying an independent and appropriate weighting on each stream of signals emitted from transmit antennas.

1.4 LTE/LTE-A

1.4.1 Why moving from LTE to LTE-A ?

As the General Background section 1.1 explained in the beginning of this chapter, 3G requirements were specified by the ITU as part of the IMT-2000 project, UMTS-HSPA, CDMA-2000 EV-DO and more recently WiMAX are the primary and official 3G technologies.

The ITU has recently issued requirements for IMT-Advanced, which constitutes the official definition of 4G. Requirements include operation in up to 40 MHz radio channels and extremely high spectral efficiency. The ITU recommends operation in up to 100 MHz radio channels and peak spectral efficiency of 15 bps/Hz in the downlink channel, resulting in a

theoretical throughput rate of 1.5 Gbps. Previous to the publication of the requirements, 1 Gbps was frequently cited as a 4G goal.

Moreover, if LTE-Advanced is compared to LTE, we can mention these benefits:

- *Spectrum efficiency*: 3 times greater than LTE.
- *Spectrum use*: The ability to support scalable bandwidth use and spectrum aggregation where non-contiguous spectrum needs to be used.
- *Latency*: From Idle to Connected in less than 50 ms and then shorter than 5 ms one way for individual packet transmission.
- *Cell edge user throughput*: twice greater than LTE.
- *Average user throughput*: 3 times greater than LTE.
- *Mobility*: Same as that in LTE
- *Compatibility*: LTE-Advanced will be compatible with LTE backwards and forwards, meaning LTE devices will operate in newer LTE-Advanced networks, and LTE-Advanced devices will operate in older LTE networks.

1.4.2 Basic LTE-A features

3GPP is addressing the IMT-Advanced requirements through LTE- Advanced with specifications mentioned into the Release 10 [3].

Figure 1.4 shows a short comparative between LTE-Advanced and the IMT-Advanced requirements.

We can also mention these following capabilities for LTE-Advanced:

- The 100 MHz spectrum aggregation is done via an aggregation of 20 MHz blocks.
- The uplink channel is MIMO of up to four transmit antennas with the UE device and allows dedicated beamforming (absent in LTE)
- The uplink channel is MIMO of up to eight by eight antennas.

Item	IMT-Advanced Requirement	LTE-Advanced Projected Capability
Peak Data Rate Downlink		1 Gbps
Peak Data Rate Uplink		500 Mbps
Spectrum Allocation	Up to 40 MHz	Up to 100 MHz
Latency User Plane	10 msec	10 msec
Latency Control Plane	100 msec	50 msec
Peak Spectral Efficiency DL[123]	15 bps/Hz	30 bps/Hz
Peak Spectral Efficiency UL	6.75 bps/Hz	15 bps/Hz
Average Spectral Efficiency DL	2.2 bps/Hz	2.6 bps/Hz
Average Spectral Efficiency UL	1.4 bps/Hz	2.0 bps/Hz
Cell-Edge Spectral Efficiency DL	0.06 bps/Hz	0.09 bps/Hz
Cell-Edge Spectral Efficiency UL	0.03 bps/Hz	0.07 bps/Hz

Figure 1.4: IMT-Advanced Requirements and LTE-Advanced Capability.

- Coordinated multipoint transmission (CoMP) with two proposed approaches: coordinated scheduling and/or beamforming, and joint processing/transmission. The intent is to closely coordinate transmissions at different cell sites, thereby achieving higher system capacity and improving cell-edge data rates.

1.4.3 Multiple access schemes

A multiple access scheme allows several terminals to share the capacity and then to transmit over the same physical media. If it is based on a multiplexing method, the same communication channel is shared between several data streams.

Multiple access schemes have several fundamental forms which can be split in time, space and frequency challenges. In LTE-Advanced, two access schemes have been selected according to the used channel mode. In downlink channel, Orthogonal Frequency Division Multiple Access (OFDMA) has been chosen and Single-Carrier Frequency Division Multiple Access (SC-FDMA) is used in the uplink channel.

Advantages and Disadvantages of each of these multiple access schemes is going to be mentioned and compared in order to explain the choice of the 3GPP.

OFDM

Advantages of OFDM

The primary advantage of OFDM consists to have a good resistance to the damaging effects of a multipath fading in the mobile channel. Actually, multipath in a radio channel causes a time delay between several beams at the receiver. This time delay introduces the notion Inter-Symbol Interference (ISI) which overlap symbols in the received signal in time. In OFDM, ISI can be avoided by inserting a guard period, also known as the Cyclic Prefix (CP), between each transmitted data symbol [20]. The CP, inserted between every symbol, has to be longer than the longest delay spread in the channel but it also reduces the data capacity of the system by the ratio of the CP to the symbol length. So, the ideal symbol length in a OFDM system is given by the reciprocal of the subcarrier spacing and is chosen to be long compared to the expected delay spread.

The other advantage of OFDM is that frequency and phase distortions in the received signal can be easily adapt. These phenomena are mainly caused by transmitter or channel imperfections. This ability also facilitates the processing required for MIMO antenna techniques such as spatial multiplexing and beamforming because signals are represented by the phase and the amplitude of subcarriers in the frequency domain. These small errors in phase and amplitude are especially susceptible to cause significant symbol demodulation errors when higher-order modulation formats (like 16QAM or 64QAM) are used.

To resume, a OFDM system transmits multiple low-rate subcarriers which are resistant to multipath phenomenon and also provide a scalable system bandwidth with associated data rates. In addition, the frequency-domain representation of signals simplifies the correction of signal errors in the receiver and reduces the complexity of MIMO implementation.

Disadvantages of OFDM

As the number of subcarriers increases, Peak to Average Power Ratio (PAPR) of signals proportionality rises with them. If an OFDM system has a large number of subcarriers, then it will have a very large PAPR since subcarriers add up coherently [21]. A high PAPR that can cause problems for amplifiers. It is not acceptable to allow these peaks to distort because it causes a spectral regrowth in the adjacent channels. The distortion can avoided by modifying

the amplifier but it will increase his cost, size and also power consumption.

A OFDM system has also a tight spacing of subcarriers which represents also main disadvantage. Actually, this tight spacing between subcarriers, created by a long duration of symbols, is set to avoid the lost efficiency created by the insertion of CP. But it also causes a loose of performances and introduces several main problems in the received signal :

- Frequency error causes interferences between the energy from one subcarrier's symbol with the next one.
- Phase noise causes similar ISI in the subcarriers but on both sides.

SC-FDM

The undesirable high PAPR of OFDM obliged 3GPP to choose a different modulation format for the LTE-Advanced uplink channel. SC-FDM is a hybrid modulation scheme which combines low PAR of single-carrier systems with the multipath resistance and flexible subcarrier frequency allocation offered by OFDM. To avoid the complex mathematical description of the SC-FDM given in [5], figure 1.5 represents a graphical comparison of the differences between OFDMA and SC-FDMA. In this figure, we can see the two different modulation schemes are mapping into time and frequency series of QPSK symbols. These symbols are composed by only four (N) subcarriers over two symbol periods.

These are QPSK data symbols so only the phase of each subcarrier is modulated and the subcarrier power remains constant between symbols. After one OFDMA symbol period has elapsed, the CP is inserted and the next four symbols are transmitted in parallel in time.

The most significant difference between the two schemes is that OFDMA transmits the four QPSK data symbols in parallel, one per subcarrier which is created the undesirable high PAR, while SC-FDMA transmits the four QPSK data symbols in series at four times the rate, we can see that the symbol length is closely related to the occupied bandwidth. Visually, the OFDMA signal is clearly multi-carrier and the SC-FDMA signal looks more like single-carrier.

To resume, SC-FDMA signal generation follows the same steps as OFDMA and provides the same advantages, like the insertion of the CP which provides a robustness against multipath. Except that in SC-FDMA, a Discrete Fourier Transform (DFT) is performed to

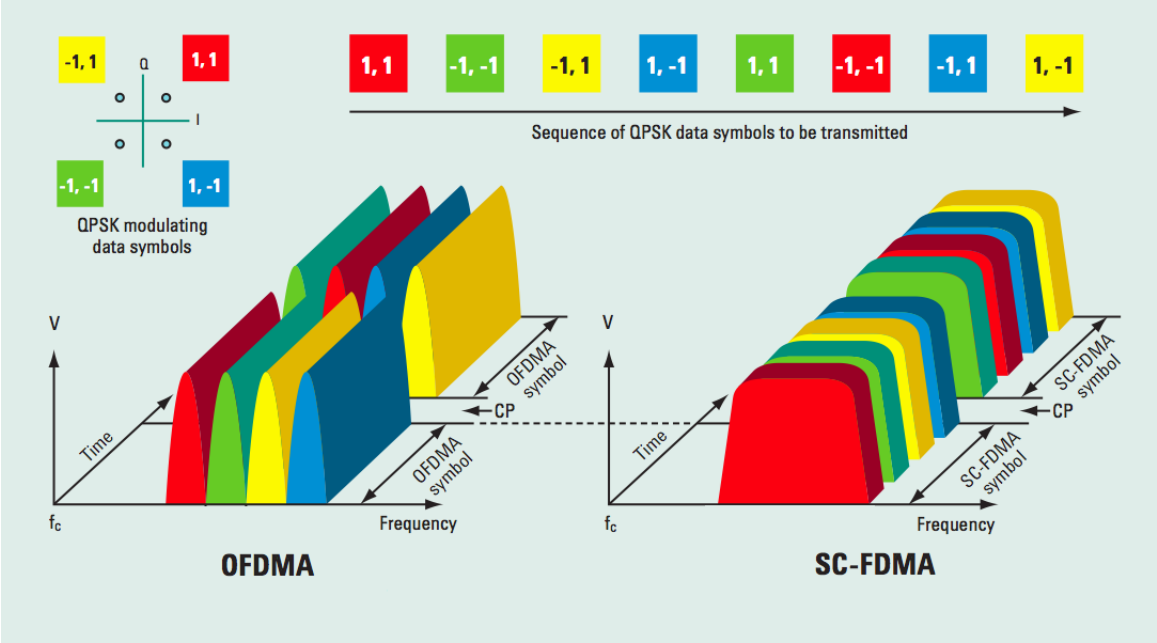

Figure 1.5: QPSK data symbols Transmission in OFDMA and SC-FDMA

transform symbols in time domain into frequency domain. And it is only after this operation that frequency domain samples are mapped to subcarriers.

In other words, SC-FDMA permits multiple subcarriers to carry each data symbol due to mapping of the symbols frequency domain samples to subcarriers contrary to OFDMA where each data symbol is carried on a separate subcarrier. Finally, SC-FDMA can be viewed as a frequency-spread (DFT-spread) OFDMA.

Chapter 2

Introduction on Precoding

This chapter is describing all the different notions which have to be known to understand the principle of precoded transmission techniques introduced in the chapter 3. Firstly, we will describe the general system of transmission from the transmitter to the receiver that is considered to implement and discuss the precoded transmission techniques. Since this project is focused on the case of the uplink channel, we don't consider the downlink channel. Secondly, transmission control schemes are explained through FDD and TDD to understand differences between LTE-Advanced frame structures.

This chapter gives also the opportunity to introduce the notion of Singular Value Decomposition (SVD) which is fundamental for the rest of the report. The mathematical aspect and the physical meaning of this technique are explained in order to tackle closed-loop and opened-loop transmission schemes.

2.1 General system of transmission for the uplink channel

In order to create a realistic scenario to simulate different precoding schemes, it is necessary to describe the general model of transmission. According to the paper [15], we used a simplified baseband MIMO SC-FDM system as it is represented in the figure 2.1

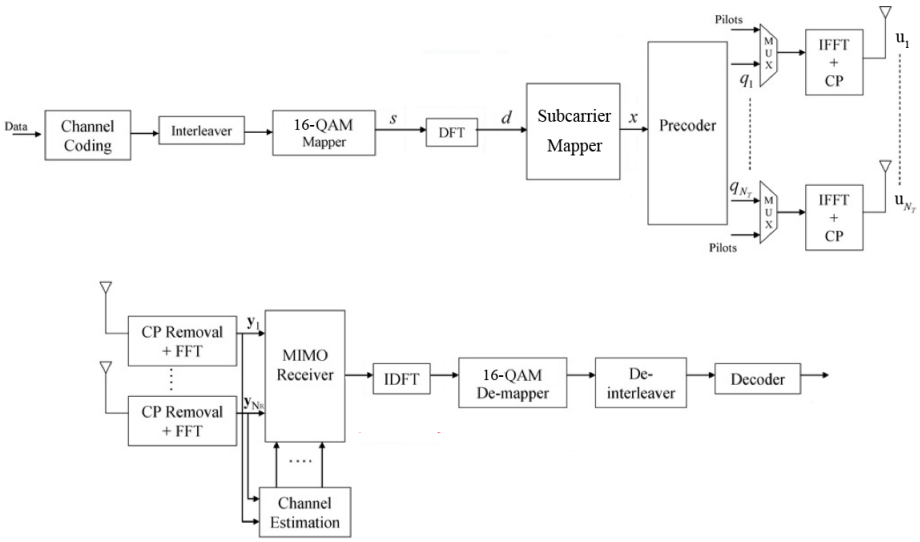

Figure 2.1: Simplified diagram of the transmission scheme

In the transmitter, the bits of the data stream are encoded, interleaved and mapped onto 16-QAM symbols given by the vector s. Then, each data symbols s is converted into the frequency domain in samples by a Discrete Fourier Transform (DFT) and represented by the vector d . After, the vector d is spread over all the subcarriers into the Subcarrier Mapper and gives the vector $x[k]$, where k designs a subcarrier, which is sent to the precoder block.

We can write the output of the precoder as :

$$q[k] = F[k]x[k] \tag{2.1}$$

where $q[k] = [q_1[k], q_2[k], \ldots, q_{N_T}[k]$ is the output of the precoder at the subcarrier k distributed over the N_T transmit antennas, and $F[k]$ is a complex precoding matrix that we define in the section 2.3.3.

Next, pilot are inserted in predefined symbols positions at each transmit antenna in order to enable channel estimation at the receiver. Finally, an IFFT is applied, gives vectors $u[k] = [u_1[k], u_2[k], \ldots, u_{N_T}[k]]$ and a CP is inserted. To simplify the model, we assume that the channel is static over the duration of an SC-FDM symbol.

The received signal at time t_0 after CP removal and Fast Fourier Transform (FFT) can be expressed like it has been introduced in the equation 1.2 :

$$y[k] = H[k]q[k] + w[k] \tag{2.2}$$

where $w[k] = [w_1(k), w_2(k), ..., w_{N_R}(k)]^T$ is the additive white Gaussian noise (AWGN) vector. $H[k]$ is the channel matrix, as it has been introduced in the equation 1.1, at a subcarrier k for a given time t_0.

The signal y_{t_0} is received by the MIMO receiver block, which performs an equalization of the received symbols with a Minimum Mean Square Error (MMSE) equalizer to compensate amplitude and phase distortions introduced by the channel. The channel estimation block permit to estimate the channel transfer function. The rest of the receiver chain performs the reverse operations of the transmitter side : Inverse Discrete Fourier Transform (IDFT), demapping, deinterleaving and decoding.

2.2 Transmission control schemes

There are many different ways of controlling the two way passage of information using two transmitters. They range in complexity from simple systems which require the least complex circuitry and give basic performance, to more complex systems which provide high levels of performance. However each scheme has its own advantages and disadvantages.

- *Simplex*: According to the definition of the American National Standards Institute (ANSI), a simplex transmission is one that can only occur in one direction. One example of this may be a broadcast system.
- *Half duplex*: This is a duplex scheme where communication is possible in two directions, but only in one direction at a given time. If one transmitter is sending data, the other one must wait until the first stops before transmitting.
- *Full duplex*: This is a scheme where transmissions can be sent in both directions simultaneously. However it is still necessary for the transmissions to be separated in some way to enable both transmissions and there are two ways to achieve this. One is to use frequency separation called FDD and the other one is to use time separation called TDD.

For each of these Full duplex modes, specific bands of frequencies have been assigned by authorities [10]. A sample of these bands is given in the figure 2.2.

Operating Band	Uplink (UL) operating band BS receive/UE transmit			Downlink (DL) operating band BS transmit /UE receive			Duplex Mode
	F_{UL_low}	–	F_{UL_high}	F_{DL_low}	–	F_{DL_high}	
1	1920 MHz	–	1980 MHz	2110 MHz	–	2170 MHz	FDD
2	1850 MHz	–	1910 MHz	1930 MHz	–	1990 MHz	FDD
3	1710 MHz	–	1785 MHz	1805 MHz	–	1880 MHz	FDD
4	1710 MHz	–	1755 MHz	2110 MHz	–	2155 MHz	FDD
5	824 MHz	–	849 MHz	869 MHz	–	894MHz	FDD
6	830 MHz-	–	840 MHz-	865 MHz	–	875 MHz-	FDD
7	2500 MHz	–	2570 MHz	2620 MHz	–	2690 MHz	FDD
8	880 MHz	–	915 MHz	925 MHz	–	960 MHz	FDD
9	1749.9 MHz	–	1784.9 MHz	1844.9 MHz	–	1879.9 MHz	FDD
10	1710 MHz	–	1770 MHz	2110 MHz	–	2170 MHz	FDD
...	...			...			...
33	1900 MHz	–	1920 MHz	1900 MHz	–	1920 MHz	TDD
34	2010 MHz	–	2025 MHz	2010 MHz	–	2025 MHz	TDD
35	1850 MHz	–	1910 MHz	1850 MHz	–	1910 MHz	TDD
36	1930 MHz	–	1990 MHz	1930 MHz	–	1990 MHz	TDD
37	1910 MHz	–	1930 MHz	1910 MHz	–	1930 MHz	TDD
38	2570 MHz	–	2620 MHz	2570 MHz	–	2620 MHz	TDD
39	1880 MHz	–	1920 MHz	1880 MHz	–	1920 MHz	TDD
40	2300 MHz	–	2400 MHz	2300 MHz	–	2400 MHz	TDD
41	3400 MHz	–	3600 MHz	3400 MHz	–	3600 MHz	TDD

Figure 2.2: Sample of operating bands for LTE-Advanced

2.2.1 Frequency Duplex Division mode

Principle

The idea of FDD is to use two different frequencies to achieve simultaneously the transmission and reception of signals. So, if the receiver is not tuned to the same frequency as the transmitter, it is possible to transmit and receive signals in the same time.

To make this operation possible, it is necessary that the frequency, or the channel separation between the transmission and reception frequencies is sufficient to enable the receiver not to be affected by the transmitter signal. This separation is shown in the figure 2.3.

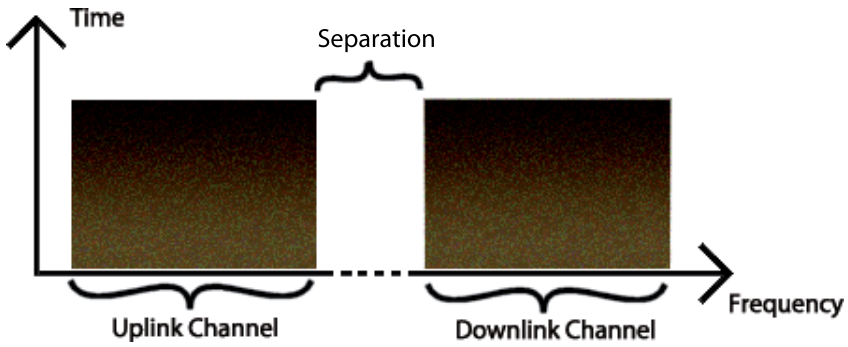

Figure 2.3: Principle of FDD Operation

But as the figure 2.2 showed it, these channels are distant from each other. There is no risk to interfere between them.

However, if the use of a FDD system allows simultaneous transmission and reception of signals, this is required two different frequency channels then, the spectrum efficiency is not optimal.

Structure of a LTE-A frame

For FDD, the 3GPP has defined a specific frame structure called *type 1*. The characteristics of this frame are set as [5]:

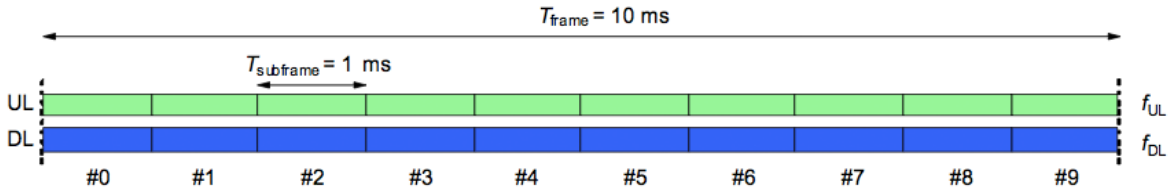

Figure 2.4: Frame structure for FDD mode

- The length of the frame is given by $T_{frame} = 10ms$ ($= 307200.T_s$) and consists of 20 slots of length $T_{slot} = 0.5ms$ ($= 15360.T_s$) , numbered from 0 to 19. Note also that

$T_s = \frac{1}{1500.2048} = 0.325\mu s$.

- A subframe is defined as two consecutive slots where subframe i consists of slots $2i$ and $2i + 1$.

The figure 2.4 gives a visual representation of these characteristics. As we can also see, 10 subframes composed a radio frame. In each 10 ms of interval, 10 subframes are available for downlink transmission and 10 subframes are available for uplink transmissions [5].

2.2.2 Time Duplex Division mode

Principle

Contrary to FDD, a TDD system uses only a single frequency, the transmission and reception share the same channel. They are spaced apart by multiplexing each signal on a time basis. TDD sends short burst of data in each direction and it introduced a time delay between each of them.

While FDD transmissions require a separation between the transmitter and receiver frequencies, TDD systems require a guard time or a Guard Period (GP) between the transmission and the reception. the GP must be sufficient to allow the signals travelling from the remote transmitter to arrive to the receiver before a transmission starts in the other direction and the receiver inhibited.

The figure 2.5 gives a visual representation of uplink and downlink subframes and also a detailed composition of a special subframe. These special subframes are specific to TDD systems and they are composed of a Uplink Pilot Time Slot (UpPTS), a Downlink Pilot Time Slot (DwPTS) and a GP [6]. In order to have a proper synchronization between each uplink and downlink subframe and then avoid interferences, a Primary Synchronisation Signal (PSS) and a Secondary Synchronization Signal (SSS) are also introduced.

To have a suitable GP, there are two main elements which have to be taken in account :

- A time allowance for the propagation delay for any transmissions from the remote transmitter to arrive at the receiver. This will depend upon the distances involved.

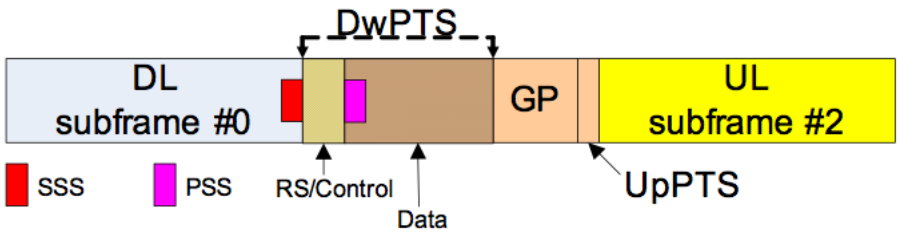

Figure 2.5: Principle of TDD Operation

- A time allowance for the transmitter/receiver to change from receive to transmit. Switching speeds can vary considerably between equipments.

Structure of a LTE-A frame

For TDD, the 3GPP has defined a specific frame structure called *type 2* [5].

As the figure 2.6 shows it, the structure of a frame is defined as:

- Each radio frame has a length of $T_{frame} = 10ms$ $(= 307200.T_s)$. It is composed of two half-frames with a length of $T_{half-frame} = \frac{T_{frame}}{2} = 5ms$ $(= 153600.T_s)$.
- Each half-frame is composed of five subframes which have a length of $T_{subframe} = 1ms$ $(= 30720.T_s)$.

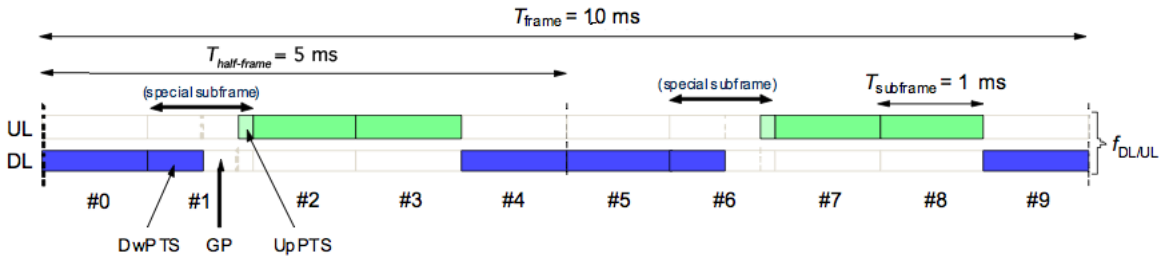

Figure 2.6: Frame structure for TDD mode

Since the uplink and downlink transmissions share the same frequency, the characteristics of this frame depend of the uplink-downlink configurations selected. The supported configurations, defined by the 3GPP [5], are listed in the figure 2.7. For each subframe, the subframe

D is reserved for downlink transmissions, the subframe U is reserved for uplink transmissions and the subframe S is the special subframe as it has been introduced in the section 2.2.2.

Note that the figure 2.6 represents the Uplink-Downlink configuration #1 according to the figure 2.7.

Uplink-downlink configuration	Downlink-to-Uplink Switch-point periodicity	Subframe number									
		0	1	2	3	4	5	6	7	8	9
0	5 ms	D	S	U	U	U	D	S	U	U	U
1	5 ms	D	S	U	U	D	D	S	U	U	D
2	5 ms	D	S	U	D	D	D	S	U	D	D
3	10 ms	D	S	U	U	U	D	D	D	D	D
4	10 ms	D	S	U	U	D	D	D	D	D	D
5	10 ms	D	S	U	D	D	D	D	D	D	D
6	5 ms	D	S	U	U	U	D	S	U	U	D

Figure 2.7: Uplink-downlink configurations in TDD

Lengths of DwPTS and UpPTS are given in the figure 2.8. The total length of DwPTS, GP and UpPTS have to be equal to $30720.T_s = 1ms$. Each subframe i is defined as two slots, $2i$ and $2i + 1$ of length $T_{slot} = 15360.Ts = 0.5ms$ in each subframe.

Special subframe configuration	Normal cyclic prefix in downlink			Extended cyclic prefix in downlink		
	DwPTS	UpPTS		DwPTS	UpPTS	
		Normal cyclic prefix in uplink	Extended cyclic prefix in uplink		Normal cyclic prefix in uplink	Extended cyclic prefix in uplink
0	$6592 \cdot T_s$	$2192 \cdot T_s$	$2560 \cdot T_s$	$7680 \cdot T_s$	$2192 \cdot T_s$	$2560 \cdot T_s$
1	$19760 \cdot T_s$			$20480 \cdot T_s$		
2	$21952 \cdot T_s$			$23040 \cdot T_s$		
3	$24144 \cdot T_s$			$25600 \cdot T_s$		
4	$26336 \cdot T_s$			$7680 \cdot T_s$	$4384 \cdot T_s$	$5120 \cdot T_s$
5	$6592 \cdot T_s$	$4384 \cdot T_s$	$5120 \cdot T_s$	$20480 \cdot T_s$		
6	$19760 \cdot T_s$			$23040 \cdot T_s$		
7	$21952 \cdot T_s$			-	-	-
8	$24144 \cdot T_s$			-	-	-

Figure 2.8: Configuration of special subframe (lengths of DwPTS/GP/UpPTS)

Uplink-downlink configurations with both 5 ms and 10 ms downlink-to-uplink switch-point periodicity are supported :

- In case of 5 ms downlink-to-uplink switch-point periodicity, the special subframe exists

in both half-frames, as the figure 2.6 shows it.

- In case of 10 ms downlink-to-uplink switch-point periodicity, the special subframe exists in the first half-frame only.

Note also that, subframes 0 and 5 and DwPTS are always reserved for downlink transmission. UpPTS and the subframe immediately following the special subframe are always reserved for uplink transmission.

2.3 Singular Value Decomposition

2.3.1 Mathematical Background

Basic Definition

Let A be a m-by-n matrix with $m \geq n$.
Then one form of the singular value decomposition of A is:

$$A = U_h \Sigma V_a^T \tag{2.3}$$

where U_h and V_a^T are orthonormal and Σ is diagonal. The indices a and h indicate matrices with aligner and hanger vectors respectively. That is $U_h^T U_h = I_m$, $V_a V_a^T = I_n$, U_h is m-by-m, V_a is n-by-n and

$$\mathbf{\Sigma} = \begin{pmatrix} \sigma_1 & 0 & \dots & 0 & 0 \\ 0 & \sigma_2 & \dots & 0 & 0 \\ \vdots & \vdots & \ddots & \vdots & \vdots \\ 0 & 0 & \dots & \sigma_{r-1} & 0 \\ 0 & 0 & \dots & 0 & \sigma_r \end{pmatrix} \tag{2.4}$$

is an m-by-n diagonal matrix (the same dimensions as A). In addition $\sigma_1 \geq \sigma_2 \geq \dots \geq \sigma_n \geq 0$. The σ_i are called the singular values of A and the number of the non-zero σ_i is equal to the rank of A. The ratio $\frac{\sigma_1}{\sigma_2}$, if $\sigma_n \neq 0$ can be regarded as a condition number of the matrix A.

It is easily verified that the singular-value decomposition can be also written as:

$$A = U_h \Sigma V_a^T = \sum_{i=1}^{n} \sigma_i h_i a_i^T \tag{2.5}$$

The matrix $h_i a_i^T$ is the outer product of the i-th row of U_h with the corresponding row of V_a. Note that each of these matrices can be stored using only $m + n$ locations rather than mn locations.

The SVD-Fundamental Theorem of Linear Algebra

In order to to show how SVD analysis is done, we will prove that:

$$Aa_i = \sigma_i h_i \tag{2.6}$$

which we call the SVD-Fundamental Theorem of Linear Algebra:

Theorem 1: For an m-by-n matrix, with $m \geq n$, $A : R_n \rightarrow R_m$ there exists an orthonormal basis $\{a_1, \ldots, a_n\}$ of R^n, obtained from the Spectral Theorem as the eigenvectors of $A^T A$ [7].

Spectral Theorem: If A is a square symmetric matrix (i.e. $A = A^T$), then there is an orthonormal basis of the column space $R(A)$ consisting of unit eigenvectors of A.

So, the theorem 1 defines :

$$(i) \qquad \sigma_i = \|Aa_i\|, \qquad i = 1, 2, \ldots, r.$$

are the non-zero singular values, where $\|$ is the Euclidean norm, and

$$(ii) \qquad h_i = \frac{1}{\sigma_i} Aa_i, \qquad i = 1, 2, \ldots, r. \quad and \quad r \leq n$$

Then, we clearly have :

$$\sigma_i h_i = \sigma_i \frac{1}{\sigma_i} Aa_i$$

So, we get the equation 2.6:

$$Aa_i = \sigma_i h_i \qquad i = 1, 2, \ldots, r.$$

From this equation, it follows that $AV_a = U_h\Sigma$ and if we multiple both sides by V_a^T, we obtain the equation 2.3 :

$$A = U_h\Sigma V_a^T \tag{2.7}$$

This theorem is used to solve systems of linear equations.

2.3.2 Channel matrix

In our case, the channel transmission scheme introduced in the section 2.1 is defined as a system of linear equations. So, we can apply the definition of SVD mentioned in the section 2.3.1.

According to the previous notations, we have now:

$$H_{t_0}[k] = U_{t_0}[k]\Sigma_{t_0}[k]V_{t_0}[k]^H \tag{2.8}$$

Notions introduced in the section 2.3.1 are still available here, the definition of each stays the same. If we adapt the notation, we have :

$U_{t_0}[k]$ is a N_R-by-N_R matrix which haves eigenvectors of $H_{t_0}[k]^H H_{t_0}[k]$ in its columns. $\Sigma_{t_0}[k]$ is a N_R-by-N_T diagonal matrix which haves eigenvalues of $H_{t_0}[k]^H H_{t_0}[k]$ and represents the channel transfer function, finally $V_{t_0}[k]$ is a N_T-by-N_T matrix which haves eigenvectors of $H_{t_0}[k]H_{t_0}[k]^H$ in its columns.

Note also that $U_{t_0}[k]$ and $V_{t_0}[k]$ are unitary matrices as it has been shown in the previous section.

2.3.3 Ideal Precoding

The SVD also allows us to go deeply into the notion of precoding mentioned in the section 2.1 with the complex precoding matrix $F[k]$.

The figure 2.9 shows the result of the SVD on the matrix channel H.

In this way, we can define the precoding matrix as :

$$F[k] = F_{t_0}[k] = \sqrt{P_{TxAnt}}\tilde{V}_{t_{\alpha 0}}[k] \tag{2.9}$$

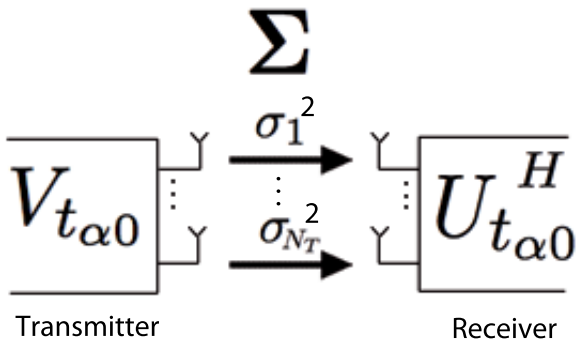

Figure 2.9: SVD Operation on the channel matrix

where $\tilde{V}_{t_{\alpha 0}}[k]$ is the matrix which contain the N_T columns of $V_{t_{\alpha 0}}[k]$ and P_{TxAnt} is a diagonal matrix of the transmit powers of each transmit antenna given by $P_1, \ldots, P_{N_T}$. We also assume that a constant total transmit power is defined as : $P_{total} = \sum_{i=1}^{N_T} P_i$.

If we use the $U_{t_0}^H[k]$ matrix as a matched filter at the receiver, the MIMO channel can be decomposed in N_T Single-Input-Single-Output (SISO) channels, as the figure 2.9 shows it. The gains of each channel defined by $\sigma_1^2, \ldots, \sigma_{N_T}^2$, are called eigenmodes.

Thanks to this approach, the capacity of the MIMO channel will increased because the intersteam interference would be removed.

2.4 Closed-loop transmission

In the section 2.3.3, we introduced the notion of precoding. But the solution is ideal and then it cannot be used in a real system. One of the main previous assumptions was that the transmitter perfectly knows the channel state before sending data.

To have a better realistic approach, we now consider that the transmitter is not aware of the channel state. However, it stays possible to get this information to compute a precoding. Thanks to a SVD, the receiver can estimate the channel frequency response and then send it to the transmitter. It is the use of this feedback information which implies the notion of closed-loop transmission.

Since this report is not focused on this aspect, we will consider it as a reference in order to

make a relevant comparison of performances with precoding techniques in open-loop transmission described in the chapter 3. Detail of this consideration for the simulations are given in the section 4.2.3.

Based on the paper [15], the closed-loop has been modelled as the figure 2.10 shows it.

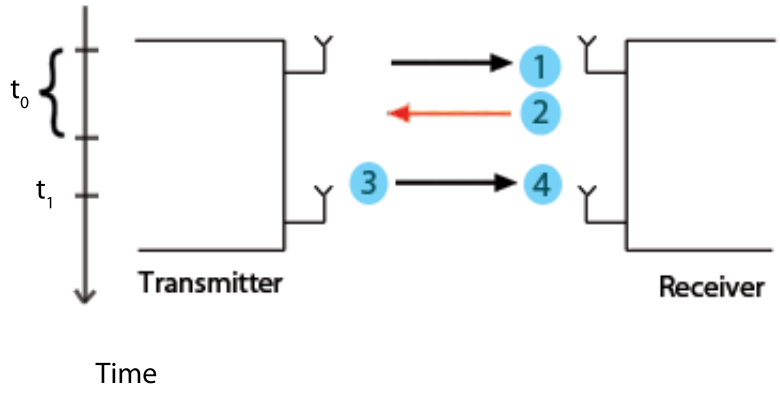

Figure 2.10: Steps of a Closed-Loop Transmission with feedback

The steps mentioned in this figure are described as followed :

1. At t_0, the eNodeB estimates the channel frequency response H_{t_0} thanks to the pilot information.
2. At t_0, the eNodeB creates the precoding matrix F_{t_0} thanks to a SVD realized on H_{t_0} and send it to the UE.
3. At t_1, the UE uses the received matrix F_{t_0} to precode the next data stream, and sends it to the eNodeB.
4. At t_1, the eNodeB makes an equalization of the channel with the MMSE equalizer, as it is defined in the equation 2.10 and after, estimates H_{t_1} thanks to the pilot information.

$$Q_{t_1}[k] = (F_{t_0}[k]^H H_{t_1}[k] F_{t_0}[k] + \frac{R_{ww}}{P_{TxAnt}})^{-1} F_{t_0}[k]^H H_{t_1}[k]^H \tag{2.10}$$

where $R_{ww} = E[w[k]w[k]^H]$ is the autocorrelation matrix of the AWGN $w[k]$ vector. We define this approach since the noise is a random process, its instantaneous realization at the receiver. cannot be know. That is why, the AWGN is estimated by its variance.

The red arrow in the figure 2.10 designs the feedback information which contains the precoding matrix F_{t_0}. This feedback is defined as the unquantified feedback. But, even if this model is more realistic than the ideal precoding defined in the section 2.3.3, it stays not feasible because it implies an infinite increase of the amount of data to send.

To correct this model, we can use codebooks as the 3GPP mentioned it. These codebooks have a limited size and contain several precoding matrices designed by an index [18]. Thanks to that, the feedback can have a limited size since only the index of the precoding matrix (chosen according to the channel estimation) has to be send. If this technique is realistic, it also implies a significant loss of performances because the codebook has a limited size which also implies a limited number of stored precoding matrices. As we said previously, this report is not focused on this aspect so we will not go into details.

Chapter 3

Precoding Techniques in Open-loop

3.1 Principle of a open-loop transmission

Open-loop transmissions do not use feedback informations as the closed-loop transmission mentioned in the section 2.4, to get an estimation of the channel. To have a relevant knowledge of this channel, an open-loop transmission scheme uses the idea of the channel reciprocity which permit TDD because both downlink and uplink are using the same frequency channel.

That is why FDD cannot be used in an open-loop transmissions since downlink and uplink channels do not used the same frequency. Each of these channels are totally different and then, they are not reciprocal.

In the following sections we will discuss about the different constraints that channel reciprocity can have and then, introduce the concept of calibration error between transmitter and receiver.

3.1.1 Channel Reciprocity

One of the main aspects of a TDD system is that uplink and downlink signals are sent over the same frequency band, as we mentioned in the section 2.2.2. If we assume configurations of antennas are symmetric and the RF chain is adequately calibrated, there is a high correlation of the fading on the signal between uplink and downlink subframes. This phenomenon is known as the channel reciprocity.

The direct benefit of this reciprocity is that if we estimate the channel in one direction, these results can be used to predict the other direction which permit to reduce the global overhead of the system. But the interference level between uplink and downlink subframes can vary significantly, that is why specifications of LTE-Advanced in TDD do not rely on the availability of channel reciprocity and allow for a full decoupling of uplink and downlink [11]. However,in cases where reciprocity is applicable, the specifications gives a large degree of freedom available to optimize the total signalling overhead.

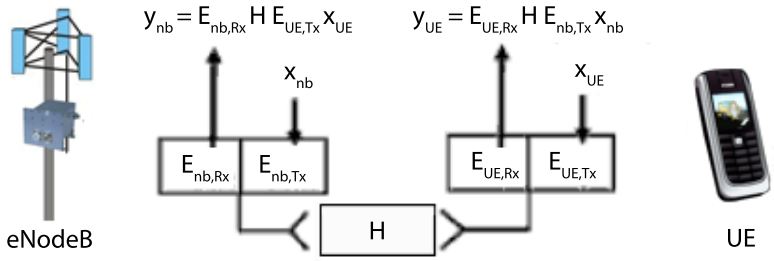

Figure 3.1: Impact from RF units to channel reciprocity

The figure 3.1 shows a simple linear model of a TDD channel which include impact from Radio Frequency (RF) chains. So, even if the channel matrix H is identical for UL and DL subframes, the channel seen by physical layer is different. Considering a typical application of channel state information (CSI), it is necessary to estimate the channel as seen by physical layer (in UL $E_{nb,Rx}HE_{UE,Tx}$). This is caused, as the section 2.1 shows it, by the fact that precoding is done only after the signal has passed through the RF parts.

To improve the channel reciprocity, it is possible to add calibration procedures between the eNodeB and the UE. If we consider this aspect, it will involve that $x_{nb} = x_{UE}$, then $y_{nb} = y_{UE}$ which required a standardized procedure.

To resume, channel reciprocity aspect can be use if the following two points are considered separately:

- Calibrated RF front-ends are required
- The CSI taken over from the reverse link should not become outdated.

3.1.2 Calibration Error

As we saw, channel reciprocity directly depends of the calibration between the transmitter and the receiver. Here, we will introduce the concept of calibration error because it is assumed that the reciprocity of a channel mainly depends for antennas which are not perfect, meaning some looses are generated and it is not physically possible to have a perfect calibration between the transmitter.

To explain quickly the causes of this error, it is due to the different IQ mixers, amplifiers and path lengths which are used at the transmitter and the receiver to separate RF chains. The most significant element which causes this phenomenon is the IQ mixer, a part of the received signal gets lost in the base-band after it [25].

This error of calibration is considered as an attenuation of the received signal since antennas are not perfectly calibrated, the mathematical aspect of this consideration is detailed in the section 4.6.4.

3.2 Blind Precoding

As it has been explained in the section 2.2.2, an UE and an eNodeB are transmitting over the same frequencies but at different time instants if TDD mode is considered. Channel reciprocity allows the possibility to preform a precoding without feedback from the eNodeB.

Here, the concept is to use the precoding matrix from the channel estimated with the previous subframe. The principle of this transmission is illustrated by the figure 3.2.

The steps mentioned in this figure are described as followed :

1. At t_0, the UE receives a subframe and computes the precoding matrix F_{t_0} from the estimated H_{t_0}.
2. At t_1, The matrix F_{t_0} is used to precode the subframe which is transmitted.
3. At t_1, The eNodeB receives the data frame and computes F_{t_1} from the estimated channel matrix H_{t_1}.

If the channel is slow time-variant, the principle of blind precoding can be considered. We define a slow time-variant channel if we have $F_{t_0} \approx F_{t_1}$. However, since we are using the

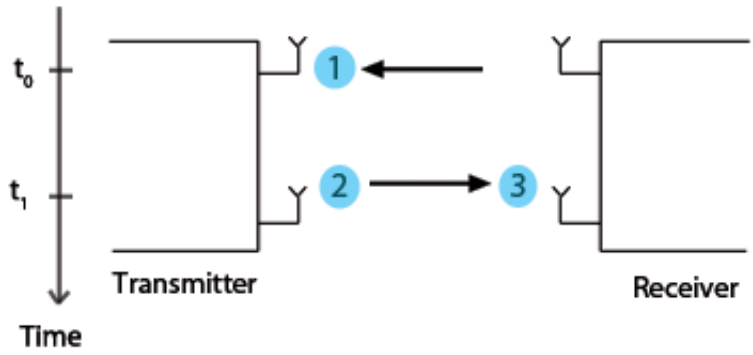

Figure 3.2: Steps of a Blind Transmission in Open-loop

SVD, even a small variation of the decomposed channel matrix H implies a huge variation of unitary matrices V and U [15]. Then we have :

$$H_{t_0} \approx H_{t_1} \quad \Longrightarrow \quad V_{t_0} \neq V_{t_1} \quad and \quad U_{t_0} \neq U_{t_1}$$

As we defined previously in the equation 2.9, the precoding matrix F directly depends of the unitary matrix V. So, we can easily deduce that in this case,

$$H_{t_0} \approx H_{t_1} \quad \Longrightarrow \quad F_{t_0} \neq F_{t_1}$$

So, the channel equalization performs at the time instant t_{t_1} by the MMSE equalizer is defined by the equation 3.1.

$$Q_{t_1}[k] = (F_{t_1}[k]^H H_{t_1}[k] F_{t_1}[k] + \frac{R_{ww}}{P_{TxAnt}})^{-1} F_{t_0}[k]^H H_{t_1}[k]^H \tag{3.1}$$

where $w[k]$ is the AWGN vector defined in the equation 2.2 and I_d is the identity matrix. So, we can easily see that if the precoding matrix $F[k]$ is outdated, the equalization cannot be perform correctly contrary to the closed-loop transmission as it is defined in the equation 2.10.

If we have a time delay $\Delta t = t_1 - t_0$ short enough, then the precoding matrix can be computed without become outdated.

3.3 Precoded Pilots

As we saw in the previous section, blind precoding is not going to work properly. In this way, we have to think about another solution to have an efficient precoding scheme. Since reference signals with predetermined amplitude and phase (pilots) are introduced in each subframes, as it is shown in the section 2.1, we have the possibility to also insert the precoding on them.

3.3.1 Principle of Pilots

Pilots are inserted in specific positions in the subframe. We assume that these positions are considered as the figure 3.3 shows it. We defined $N_{symb} = 1, 2, \ldots, 14$ as the position of each symbol.

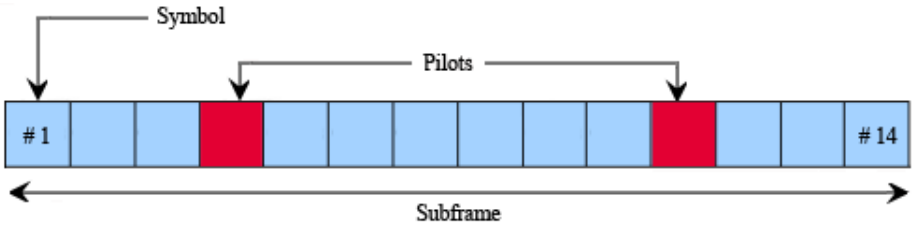

Figure 3.3: Positions of pilots in the subframe

Considering two antennas are transmitting in SM, the subframe is composed as this figure 3.4 shows it.

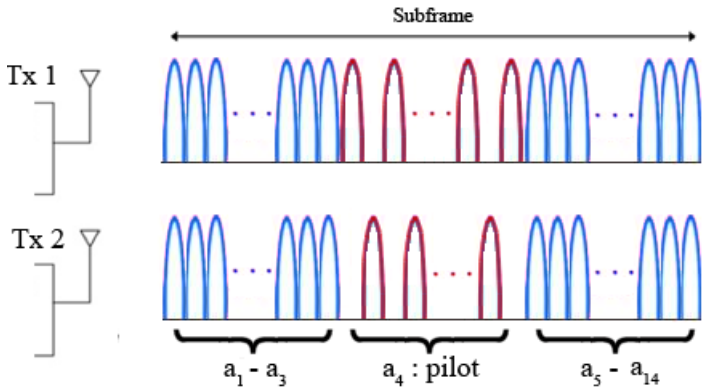

Figure 3.4: Transmit subframe with alternated pilots

where Tx 1 and Tx 2 are the first and the second transmit antennas, respectively. $a_{N_{symb}}$ designs symbols where $N_{symb} = 1, \ldots, 14$. Samples in blue design data symbols and samples in red design the pilot. As we can see, values are alternated between each antenna according to a predefined pattern. Since the channel estimation is based on pilots, this alternation permits to avoid interferences in the channel estimation process.

Note also that pilots are particularly useful when higher-order modulation formats, like 16-QAM, are used. These modulations can generated erroneous symbol demodulation with even small errors in phase and amplitude.

Then, the received signal, as it has been defined by the equation 2.2 in a general way, depends also of pilots:

$y[k] = H[k]V[k]q[k] + w[k] \qquad if\ N_{symb} = \{1, 2, 3, 5, 6, 7, 8, 9, 10, 12, 13, 14\}$

$y_p[k] = H[k]p[k] + w[k] \qquad if\ N_{symb} = \{4, 11\}$

where $p[k]$ designs the pilot symbol and $y_p[k]$ is the received signal of this symbol. When the estimation, based on the Wiener Filter (WF) [19], is performed on y_p as the figure 3.5 shows it.

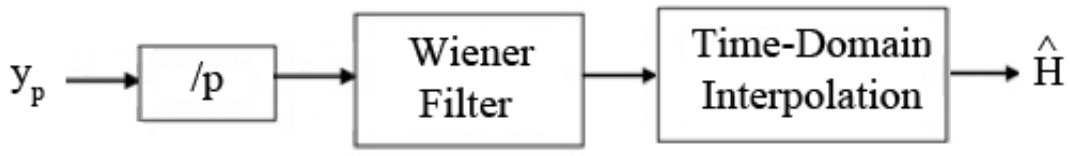

Figure 3.5: Channel Estimation on Pilots

where $\hat{H}$ is the estimated channel matrix with the additive AWGN defined as: $\hat{H} = \frac{Hp+w}{p} = \tilde{H} + \tilde{w}$

Actually, these pilots were already inserted with the blind precoding technique. So, we know it is not efficient enough to have a good precoding performance.

3.3.2 Precoding on Pilots

The idea of precoded pilots transmission, as the name mentioned it, is to insert the precoding also on pilots. Since the equation 2.1 gives the output of precoder as:

$$q[k] = F[k]x[k]$$

Then, considering the precoding matrix defined in the equation 2.9, we have:

$$q[k] = \sqrt{P_{TxAnt}}\tilde{V}[k]x[k]$$

where $\tilde{V}[k]$ is the matrix which contain the N_T columns of $V[k]$. Since the CW-to-layer mappers maps samples onto a single layer, a rank-1 precoder is used. So, we can write the matrix $\tilde{V}$ as:

$$\tilde{\mathbf{V}} = \begin{pmatrix} V_0 \\ V_1 \end{pmatrix} \tag{3.2}$$

where V_0 andV_1 are the precoding values applies on the first and the second transmit antennas, respectively. Actually, these value are given by the first column of V which is related to the strongest eigenvalue of the channel, as it is demonstrated in the section 2.3.1.

So, the received signal is now written as:
$y[k] = H[k]V[k]q[k] + w[k] \qquad if\ N_{symb} = \{1, 2, 3, 5, 6, 7, 8, 9, 10, 12, 13, 14\}$
$y_p[k] = H[k]V[k]p[k] + w[k] \qquad if\ N_{symb} = \{4, 11\}$

It is easy to understand that now, the estimation of the channel is now based on the joint matrix $H_{eq} = HV$ instead of H. Then, the equalization based on a MMSE equalizer, as it is defined in the equation 3.1, is written as:

$$Q[k] = (H_{eq}[k]^H H_{eq}[k] + \frac{R_{ww}}{P_{TxAnt}})^{-1} H_{eq}[k]^H \tag{3.3}$$

Since, the aim of the equalizer is to remove the effect of the channel on the transmit data sequences, it corrects phase and amplitude effects and also inter-stream interference if a MIMO system is used. Then, the input of this equalizer is now the equivalent channel matrix which included the precoding matrix and the channel matrix. However, we know that a MMSE equalizer performs well in case of no precoded transmission, and similar behaviour is expected for the equivalent channel matrix H_{eq} [16]. So, the channel transfer function is directly estimated without problems of out-dating known in blind precoding.

On the other hand, this precoding implies a correction in amplitude and phase which has an direct influence on channel statistics used to estimate the channel. Then, if precoding is applied on each subcarrier, these statistics may be forced and the precoding may not be so efficient. In order to evaluate the impact of this influence, the length of the precoding has to be considered. We defined this evaluation in the section 4.6.5.

Moreover, by precoding on the amplitude and the phase of pilots, an instantaneous power imbalance between the amplifiers is created .

If we consider the power allocation issued by power amplifiers as a numerical random variable then, the distribution is this variable will be spread out. It implies a very high complexity in the conception of the power amplifier block in the transmitter. In order to simplify it, the precoding can be apply only on the phase of signals.

3.4 Phase based precoding

The phase based precoding keeps the concept of precoded pilots but as we explained previously, the precoding is made only on the phase of the signal.

The precoding matrix $\tilde{V}$ is a complex matrix that we can write as:

$$\tilde{\mathbf{V}} = \begin{pmatrix} \alpha_1 + i\beta_1 \\ \alpha_2 + i\beta_2 \end{pmatrix} \Longleftrightarrow \tilde{\mathbf{V}} = \begin{pmatrix} \sqrt{\alpha_1^2 + \beta_1^2} \mathrm{e}^{jarctg(\frac{\beta_1}{\alpha_1})} \\ \sqrt{\alpha_2^2 + \beta_2^2} \mathrm{e}^{jarctg(\frac{\beta_2}{\alpha_2})} \end{pmatrix}$$

Then, we define $\tilde{V}_\varphi$ as the precoding matrix based on the relative phase of $\tilde{V}$ as:

$$\tilde{\mathbf{V}}_\varphi = \begin{pmatrix} \frac{\mathrm{e}^{jarctg(\frac{\beta_1}{\alpha_1})}}{\mathrm{e}^{jarctg(\frac{\beta_1}{\alpha_1})}} \\ \frac{\mathrm{e}^{jarctg(\frac{\beta_2}{\alpha_2})}}{\mathrm{e}^{jarctg(\frac{\beta_1}{\alpha_1})}} \end{pmatrix} \Longleftrightarrow \tilde{\mathbf{V}}_\varphi = \begin{pmatrix} 1 \\ \mathrm{e}^{j\varphi} \end{pmatrix}$$

where φ is the relative phase defined as : $\varphi = arctg(\frac{\beta_2}{\alpha_2}) - arctg(\frac{\beta_1}{\alpha_1})$.

Since, we based the precoding only on the phase, distortions in amplitude are not going to be corrected properly. So, the received signal with phase based precoding will have a worse equalization than the received signal with the precoded pilots technique. Since, the principle is basically the same, performances of phase based precoding are excepted to be worse than precoded pilots technique but the distribution of power allocation of transmit antennas is expected to be very much tighten.

As we introduce in the section 4.6.3, the distribution is going to be evaluated with the Cumulative Distribution Function (CDF). We also evaluate the length of precoding on subcarriers to quantify its impact and have a point of comparison with precoded pilots technique.

Chapter 4

Scenario

In this chapter, we introduce scenario that we considered to run the simulations. Moreover, in order to create relevant comparisons and a proper evaluation of each precoding techniques mentioned in the chapter 3, it is necessary to take in account the influence of calibration error and size of precoding on these techniques. The mathematical aspect of these parameters is explained in this chapter.

4.1 Assumptions

As the title of this report suggested it, we evaluate performances of different precoding techniques in TDD. In this way, we assume the following points.

4.1.1 Single-User MIMO

All the following scenario are in a SU-MIMO configuration. We consider that the multiple antennas of the eNodeB are physically connected to each UE. This assumption permits to avoid all the problems linked to MU-MIMO configurations like spatially distributed transmission resources between users.

As we mentioned previously, the number of transmit antennas in a LTE-Advanced uplink channel is up to four. We chose to limit the number of these antennas to two for the following

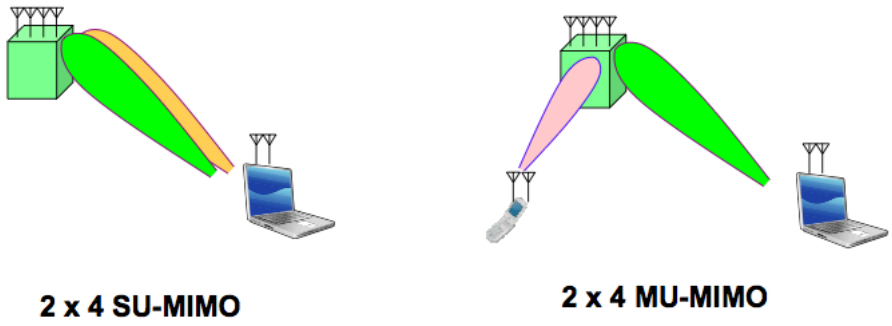

Figure 4.1: SU-MIMO and MU-MIMO

scenario, this limitation is also one of the assumptions of 3GPP Self-evaluation of LTE-Advanced uplink transmission [24]. However, we evaluate the influence of the number of receive antennas with 2-by-2 and 2-by-4 configurations.

4.1.2 Bandwidth

LTE-Advanced has the ability to use a bandwidth up to 20 Mhz (and up to 100 Mhz, if the bandwidth aggregation is used [24]), we chose to use a bandwidth of 5 Mhz for the following scenario. This assumption does not have impact on the pertinence of results but according to 3GPP TS 36.104 Technical report, the resource configuration directly depends of the bandwidth selected as the figure 4.2 shows it.

Channel bandwidth [MHz]	1.4	3	5	10	15	20
Number of resource blocks (N_{RB})	6	15	25	50	75	100
Number of occupied subcarriers	72	180	300	600	900	1200
IDFT(Tx)/DFT(Rx) size	128	256	512	1024	1536	2048
Sample rate [MHz]	1.92	3.84	7.68	15.36	23.04	30.72
Samples per slot	960	1920	3840	7680	11520	15360

Figure 4.2: Resource Configuration

4.1.3 Structure of subframes

In order to evaluate the uplink channel, we assume that only UL subframes are transmitted. Special and Downlink subframes, which are specific to TDD mode, as it has been introduced in the section 2.2.2 are not considered.

The frame structure in TDD detailed in the section 2.2.2, is constituted of 2 time slots for each one subframe. We assume that each of these time slots contains 7 SC-FDMA symbols [12] since we use CP with a normal length. The justification of the use of normal CP is given in the section 5.1.1 becuase it directly depends on the channel modelling.

To illustrate these assumptions and the description made in the section 2.1, the figure 4.3 gives a visual representation between symbols (time) and subcarriers (frequency): each symbols into a time slot is spread over all the subcarriers in order to be send over the channel.

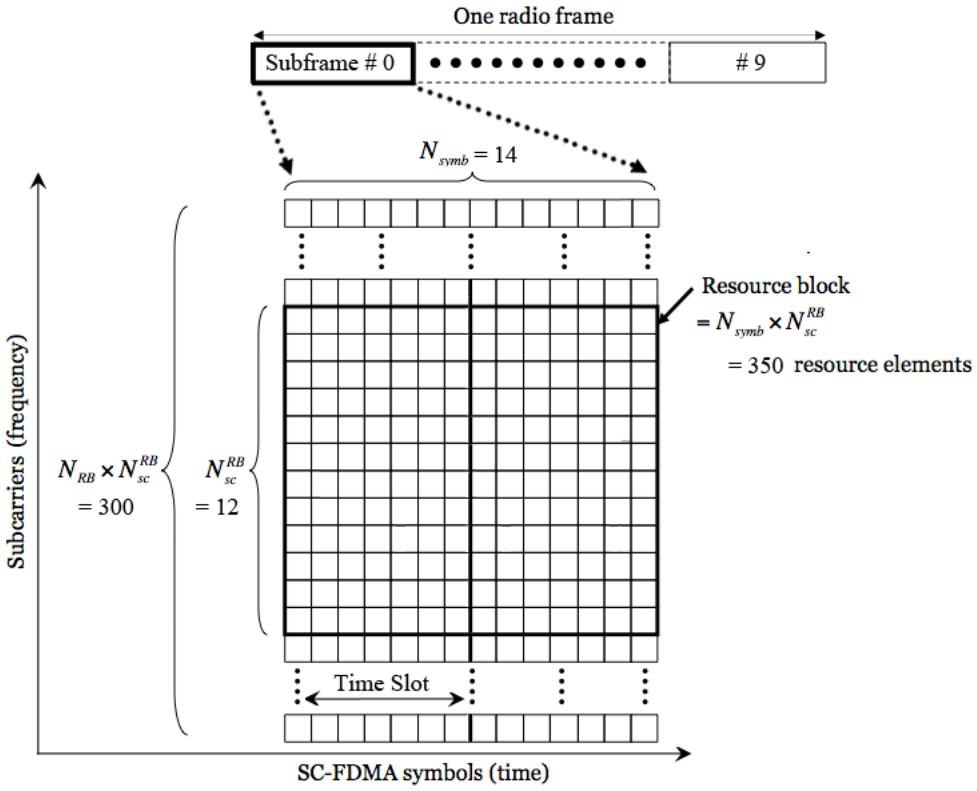

Figure 4.3: Repartition of symbols over subcarriers

4.2 Scenario A : References

Since the performance of precoding techniques is evaluated, it is necessary to have references in order to do relevant comparisons. According to the different scenario evaluated, several references have to be defined.

4.2.1 Configuration 1x2

This configuration means that one transmit antenna and two receive antennas are used. So, we have a Single Input Multiple Output (SIMO) transmission. It is a reference for scenario with a 2-by-2 antennas system. It gives the opportunity to evaluate the gain earned for each precoding technique since a SIMO configuration cannot enable precoding (only one transmit antenna).

4.2.2 Configuration 1x4

As the previous scenario, this configuration has a SIMO transmission. It is used as a reference to scenario with a 2-by-4 antennas system.

4.2.3 Closed-loop transmission with unquantized feedback

Closed-loop transmission defined in the section 2.4 mentioned how the feedback is used to improve performances of transmission. We consider an unquantified feedback in order to have the best performance we can have. Moreover, the precoding is applied on each subcarrier.

If the previous scenario in sections 4.2.1 and 4.2.2 give a relevant comparison to evaluate the amount of gain earned, this scenario gives the upper edge, meaning performances of precoding techniques in open-loop transmission cannot be better than this scenario. It is due to the unquantified feedback which gives to the transmitter an extensive knowledge of the channel compare to others.

4.3 Scenario B : Blind Precoding

The principle of blind precoding transmission explained in the section 3.2 gives the expectation that this technique will provide very low performances or even worst. So, in order to verify this expectation NB and WB precoding are going to be evaluate for this precoding technique.

4.4 Scenario C : Precoded Pilots

Precoded pilots technique in a open-loop transmission is the aim of this project. That is why this scenario has been chosen to evaluate the influence of calibration error and number of receive antennas in addition to WB and NB precoding. To resume, the figure 4.4 shows which scenario are going to be evaluate with this precoding technique.

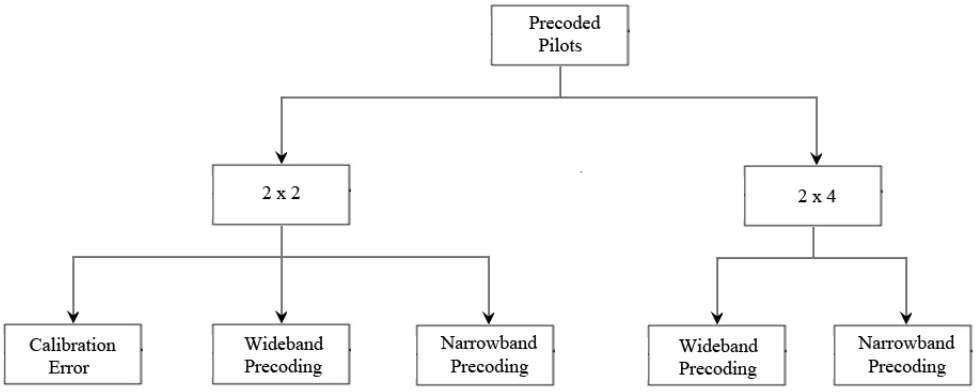

Figure 4.4: Scenario with precoded pilots technique

4.5 Scenario D : Phase based precoding

This scenario is going to evaluate the efficiency of phased based precoding compared to precoded pilots. Since we only based the precoding on the phase of pilots, we have to except a loss of performance. However, a relevant power balance between transmit antennas can be excepted as it is explained in the section 3.4.

Like blind precoding, WB and NB precoding are going to be evaluated. In addition,

the power balance of transmit antenna is also evaluated with the Cumulative Distribution Function (CDF) as it is introduced in the section 4.6.3.

4.6 What do we evaluate?

All different scenarios are now defined but to compare them it is necessary to introduce some notions and tools as it is shown in the sections from 4.6.1 to 4.6.3.

The mathematical aspect of calibration error, wideband and narrowband precoding is also introduced. These considerations are used in order to compute simulations explained in the chapter 5.

4.6.1 Spectral Efficiency

Spectral Efficiency is defined by the information rate that can be transmitted over a given bandwidth. This notion allows to measure how efficient is the transmission in a limited frequency spectrum. More specifically, we evaluated the average rate of successful message delivery over the channel, also called throughput.

The spectral efficiency is given in bits per second per Hertz per cell. Since, we consider only one cell in scenario, we measure it in bps/Hz and defined it as :

$$\eta = \frac{R}{B_w} \tag{4.1}$$

where η is spectral efficiency (bps/Hz), R is the data rate (bps) and B_w is the channel bandwidth (Hz). A detailed description of the spectral efficiency computation is given in the paper [26].

4.6.2 Block Error Rate

3GPP defines Block Error Ratio (BLER) [2] as follows:

> A Block Error Ratio is defined as the ratio of the number of erroneous blocks received to the total number of blocks sent. An erroneous block is defined as a Transport Block, the Cyclic Redundancy Check (CRC) of which is wrong.

So, a transport block is considered as an erroneous block when one bit of the block is not properly received. This verification is efficiently (meaning quickly) done by the CRC.

4.6.3 Cumulative Distribution Function

The Cumulative Distribution Function (CDF) is used to have a graphical representation of the power allocation of each transmit antenna. This allows us to have a significant representation of the comparison between the Precoded Pilots Technique and the Phase Based Precoding Technique.

As we mentioned in the section 3.4, we introduced the Phase Based Precoding Technique to avoid a widely distribution of the power allocation between each transmit frame.

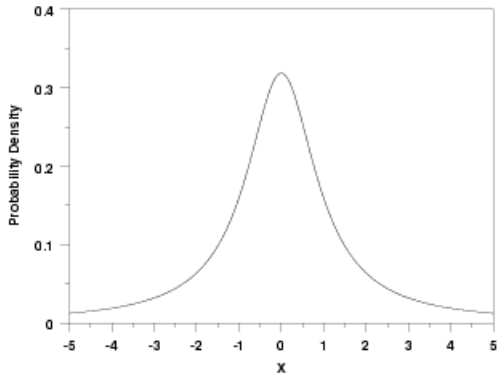

Figure 4.5: Example of a PDF

If we consider a generic example of the Probability Density Function (PDF) given by the figure 4.5. We can define the CDF as follows in the section 4.6.3.

Definition

Let X be a numerical random variable. It is completely described by the probability for a realization of the variable to be less than x for any x. This probability is denoted by $F(x)$:

$$F(x) = P\{X \leq x\} \tag{4.2}$$

$F(x)$ is the CDF of the variable X. It can be regarded as the proportion of the population whose value is less than x. The CDF of a random variable is clearly a monotonously increasing

(or more precisely, non decreasing) function from 0 to 1. A generic representation of this function

The two events $X \leq x$ and $X > x$ are mutually exclusive. Therefore :

$$P\{X \leq x\} + P\{X > x\} = 1$$

and

$$P\{X > x\} = 1 - F(x)$$

More generally, for any two numbers a and b with $a < b$, we have :

$$P\{a < X \leq b\} = F(b) - F(a) \tag{4.3}$$

Relationship between the PDF and the CDF

The relationship between the PDF and the CDF is given by :

$$P\{a < X \leq b\} = \int_a^b p(x)\,dx \tag{4.4}$$

The cumulative distribution function $F(x)$ is then continuous, and moreover its derivative $\frac{dF(x)}{dx}$ is given by the PDF $p(x)$. Then, we have the equation 4.5 represented by the figure 4.6

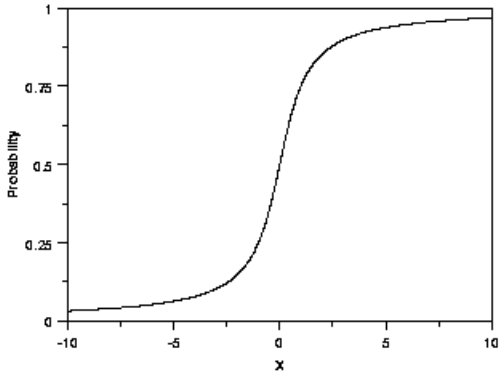

Figure 4.6: Example of a CDF

:

$$F(b) - F(a) = \int_a^b p(x)\,dx \tag{4.5}$$

As we can see a widely probability distribution given a widely cumulative distribution. If the power allocation of each antenna between the transmission of each frame does not change a lot we can excepted a narrow CDF around the mean value of the probability distribution.

4.6.4 Calibration Error

For UE, we note the transmitted signal without calibration s_n^{UE} where $n = 1, 2, \ldots$.
Then, we consider the transmitted signal with calibration error is given by equations 4.6 and 4.7 [4]:

$$|\underline{s_n^{UE}}| = 10^{\frac{20log|s_n^{UE}|+U[-\Delta_a,\Delta_a]}{20}} \tag{4.6}$$

and :

$$arg(|\underline{s_n^{UE}}|) = arg(|s_n^{UE}|) + U[-\Delta_\varphi, \Delta_\varphi] \tag{4.7}$$

In the same way, the received signal without calibration is written r_n^{UE}, so the received signal with calibration error is given by equations 4.8 and 4.9:

$$|\underline{r_n^{UE}}| = 10^{\frac{20log|r_n^{UE}|+U[-\Delta_a,\Delta_a]}{20}} \tag{4.8}$$

and :

$$arg(|\underline{r_n^{UE}}|) = arg(|r_n^{UE}|) + U[-\Delta_\varphi, \Delta_\varphi] \tag{4.9}$$

Where $arg(x)$ is the phase of x and $|x|$ is the modulus of x, $U[x, y]$ is the uniform distribution between x and y, Δ_a is the calibration error of amplitude (in dB) and Δ_φ is the calibration error of phase (in degree).

Considering that calibration error causes a degradation of performance. This degradation is going to be evaluated even if we can excepted a negligible loss of the performance [4].

4.6.5 Size/Length of Precoding

As the equation 2.1 mentioned it, we considered $x[k]$ and $q[k]$ as the input and the output of the precoder, respectively. They contain subcarriers which can be described by an amplitude and a phase.

Subcarriers are obtained from a DFT of symbols. This operation can be described by the equation 4.10 according to the notations defined in the section 2.1.

$$d_n[k] = \sum_{i=0}^{N\_1} s_i \mathrm{e}^{\frac{-j.2.\pi.i.n}{N}} \tag{4.10}$$

where N is the order of the DFT and $n = 1, 2, \ldots, N-1$.

After the application of the IFFT, if precoding is not considered, then transmit subcarriers can be written as: So, we have :

$$u_m[k] = \sum_{i=0}^{N_{IFTT}-1} x_i \mathrm{e}^{\frac{j.2.\pi.i.m}{N}} \tag{4.11}$$

where $u_m[k]$, with $m = 0, 1, 2, \ldots, N_{IFFT} - 1$, represents the transmitted signal after the IFFT and x represents the signal mapped over all the subcarriers, N_{IFTT} is the order of the IFTT operation (and FTT operation at the receiver) determined in the section 5.1.

In order to quantify the size (or the length) of precoding, notions such as NarrowBand (NB) and WideBand (WB) have to be defined.

WideBand Precoding

A WB Precoding means that all the subcarriers are precoded by the same value of the precoding matrix $F[k]$ as the figure 4.7 illustrates it and it is defined as :

$$F[k] = F_0$$

where F_0 is computed from the SVD of the averaged channel response.

Then, the output of the precoder can be written as:

$$q[k] = F_0.x[k]$$

So, we have from the equation 4.11:

$$u_m[k] = F_0 \sum_{i=0}^{N_{IFTT}-1} x_i[k] \mathrm{e}^{\frac{j.2.\pi.i.m}{N}} \tag{4.12}$$

In this case, precoding just multiply the transmit subcarriers by a factor F_0. It shows that precoding does not force channel statistics contrary to the NB precoding explained in the next section.

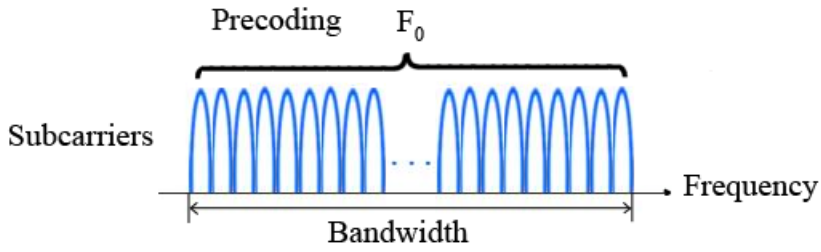

Figure 4.7: Precoding applies in Wideband

NarrowBand Precoding

Precoding in NB means that each subcarrier is precoded by different values of the precoding matrix $F[k]$, as the figure 4.8 illustrates it and it is defined as :

$$F[k] = \{F_1, F_2, \ldots, F_{N_{sub}}\}$$

where $\{F_1, F_2, \ldots, F_{N_{sub}}\}$ are computed from the SVD of the channel response and $k = 1, 2, \ldots, N_{sub}$ is the number of subcarriers.

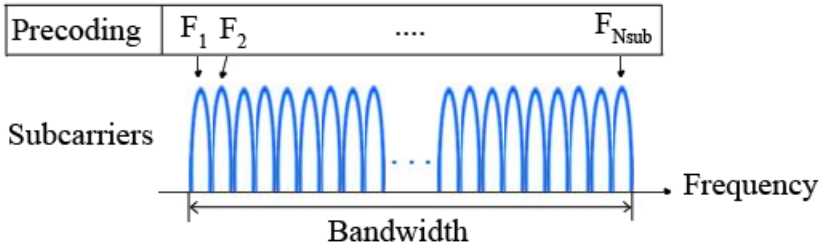

Figure 4.8: Precoding applies in Narrowband

Then, the output of the precoder is expressed as:

$$q[k] = F[k].x[k]$$

So, we have from the equation 4.11:

$$u_m[k] = \sum_{i=0}^{N_{IFTT}-1} q_i[k] \mathrm{e}^{\frac{j.2.\pi.i.m}{N}} \tag{4.13}$$

where N_{IFTT} is the order of the IFTT operation (and FTT operation at the receiver) determined in the section 5.1 and $m = 0, 1, 2, \ldots, N_{IFFT} - 1$.

Contrary to WB Precoding, considering NB permits to have a specific precoding matrix for each subcarriers. So, the precoding is supposed to be more efficient than in WB and the maximal gain is improved. So, we can expected better results in NB precoding than in WB precoding.

However, precoding in NB tends to modify randomly channel statistics since a different value of the precoding matrix is applies on each subcarrier. So, since the channel estimator selected is the WF, it directly depends of the receive correlation matrix [19] defined by: $R_{YY} = E[H.H^{H]}$, where $E[.]$ the expectation operator. It becomes obvious that if the channel statistics are randomly modified, the channel cannot be estimate properly by the WF filter.

Moreover, when NB precoding is used, the processing at the transmitter increases the PAPR of SC-FDM symbols [14] and both closed-loop and open-loop transmission are concerned. Low PAPR is the main advantages of SC-FDMA as it mentioned in the section 1.4.3 and it also one of the requirement for the uplink channel.

In order to have a relevant comparison, the Complementary Cumulative Distribution Function (CCDF) of the PAPR is evaluated. CCDF represents the opposite probability of CDF given by the equation 4.2 and it is defined as :

$$F_c(x) = P(X > x) = 1 - F(x) \tag{4.14}$$

It shows how often a random variable is above a particular level. In this case, it shows the probability of an SC-FDM frame exceeding a given PAPR following the equation:

$$CCDF(PAPR(x)) = P_r(PAPR(x) > PAPR_0)$$

The figure 4.9 extracted from the paper [14] shows the impact of a NB precoding compared to a WB precoding on SC-FDM symbols in a bandwidth of 10 MHz with a 16-QAM modulation.

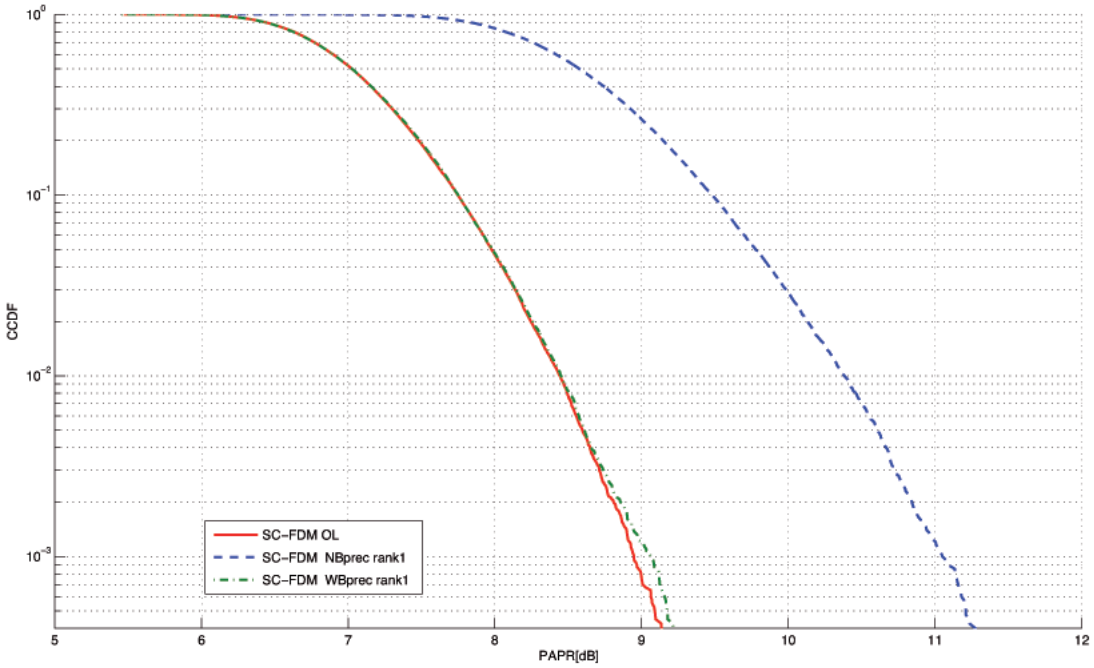

Figure 4.9: PAPR of Narrowband and Wideband Precoding

As we can WB precoding have a very low influence on the PAPR of symbols contrary to the NB precoding. So, even if NB precoding has a spectral efficiency and a BLER with higher values in gain compared to WB precoding, this technique cannot be chosen as a solution to precode the symbols.

Chapter 5

Simulations

5.1 Parameters of simulation

Simulations have been made in the following parameters mentioned in the figure 5.1:

General Parameters	
MCS settings	16-QAM
Effective Coding Rate	1/2
Channel model	TU2O
Channel Estimation	Wiener Filter
Speed	3 kmph
Physical Layer Parameters	
Transmission Technique	SC-FDMA
Equalizer	MMSE
FFT Size	512
Number of symbols per slot	7
Length of CP (μs)	7.81 4.67 4.67 4.67 4.67 4.67 4.67
System Bandwidth	5 MHz
Sampling Rate	7.68 MHz
Number of subcarriers	300
Subcarrier spacing	15 kHz
Subframe duration	1 ms
MIMO Parameters	
Scheme	Spatial Multiplexing
Type	Full-Diversity

Figure 5.1: Parameters of Simualtion

5.1.1 Channel Modelling

The multipath channel is modelled as a Typical Urban channel with a power delay profile (PDP) of 20 paths (TU20) in order to have a realistic approach [22]. It gives the intensity of a signal received as a function of time delay between multipath beam arrivals as it is shown in the figure 5.2. Note also that the path loss and fading are modelled as AWGN noises.

Number of path	TU 20	
	Delay (ns)	Power (dB)
1	0	-5.7
2	217	-7.6
3	512	-10.1
4	514	-10.2
5	517	-10.2
6	674	-11.5
7	882	-13.4
8	1230	-16.3
9	1287	-16.9
10	1311	-17.1
11	1349	-17.4
12	1533	-19.0
13	1535	-19.0
14	1622	-19.8
15	1818	-21.5
16	1836	-21.6
17	1884	-22.1
18	1943	-22.6
19	2048	-23.5
20	2140	-24.3

Figure 5.2: Typical Urban Channel Power Delay Profile

It also permits to justify the use of normal CP length inserted before each symbols :

As it is defined in the figure 5.1, the time duration of a CP (except the first one) is equal to $4.69\mu s$. Since the channel is modelled with a delay profile of 20 paths, the longest time delay given the figure 5.2 and equal to $2.14\mu s$ is shorter than the CP. That is why extended

CP are not required for this modelling, normal CP permit to avoid any ISI between symbols.

5.2 Results

In this section, all the results of simulations are presented. A comparison is made between the evaluated configuration and the adapted reference. In this way, we are going to evaluate :

- The maximal gain based on the spectral efficiency
- The gain based on a 10 % BLER threshold

5.2.1 Blind Precoding

As we mentioned in the section 3.2, if the time delay $\Delta t = t_1 - t_0$ is too extended, we do not excepted an efficient precoding with this technique. However, we assume a realistic time delay between each frame equal to $10ms$. So, we can properly performance of this technique with a realistic approach.

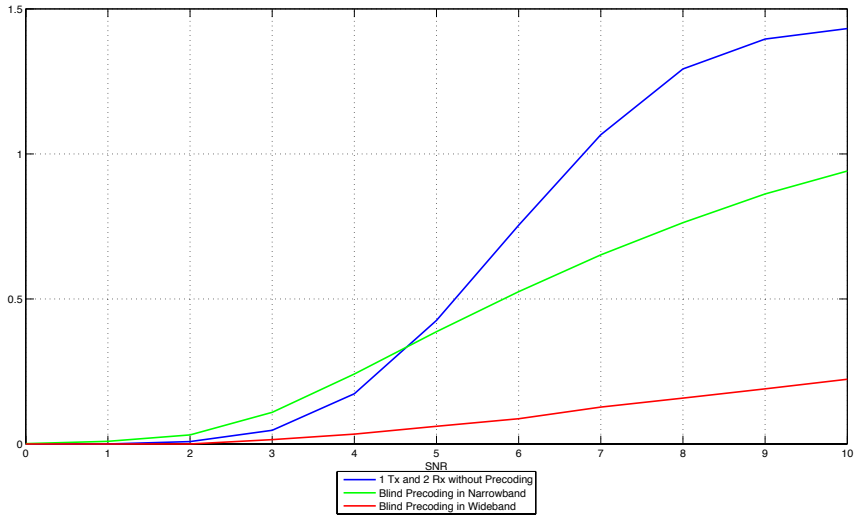

Figure 5.3: Spectral Efficiency of a Blind Precoding - Wideband vs Narrowband

The spectral efficiency gives a maximal gain of 0.068 dB if we consider the blind precoding in narrowband and 0 if we consider the curve in wideband. However, these values are not relevant at all since the maximal spectral efficiency cannot reach the spectral efficiency of a SIMO system without precoding.

Exceptions are confirmed, blind precoding in an open-loop transmission do not improve the gain, even worst it diminishes performances.

Note also that precoding in narrowband is less bad than precoding in wideband as we excepted in the section 4.6.5. However, both of these precoding are still not usable.

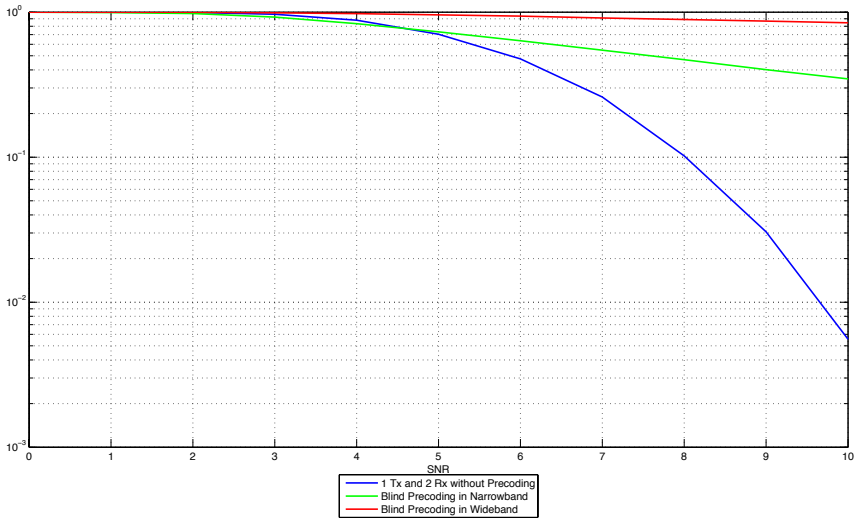

Figure 5.4: Block Error Rate of a Blind Precoding - Wideband vs Narrowband

BLER results confirm previous ones. None of these curves, neither in NB, gives measurable values at a 10 % BLER threshold since they are not enable to reach it.

This precoding can definitively not be used in an open-loop transmission.

5.2.2 Precoded Pilots

In this section, results of the performance evaluation with the precoded pilots technique are presented. As we defined in the section 4.4, in addition of the evaluation of the length of precoding, this scenario is used to estimate the impact of calibration error on performances. We also present a comparison of performances between a 2x2 (two transmit antennas and two receive antennas) system and a 2x4 (two transmit antennas and four receive antennas) system.

Wideband vs Narrowband

The following graphs show the comparison between a WB precoding and a NB precoding with the precoded pilots technique in a 2x2 system.

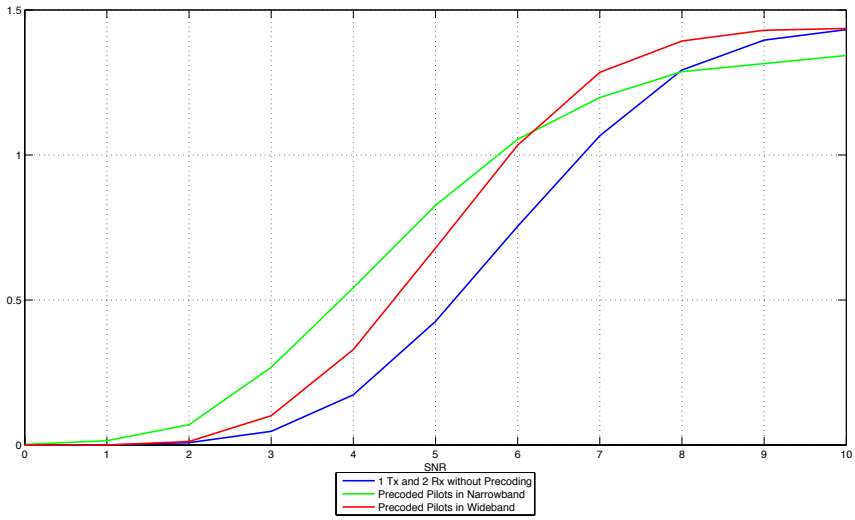

Figure 5.5: Spectral Efficiency of Precoded Pilots - Wideband vs Narrowband

The spectral efficiency gives a maximal gain of $0.400dB$ if we compare the NB precoding with the SIMO reference system. The maximal gain with the WB precoding is up to $0.280dB$.

At a low Signal-to-Noise Ratio (SNR), NB precoding looks more efficient than WB precoding, since the precoding is applied on each subcarrier. However, the forcing of the channel

statistics shows its influence once a higher SNR is considered. NB precoding is not able to reach to the same maximal value of the reference system in time.

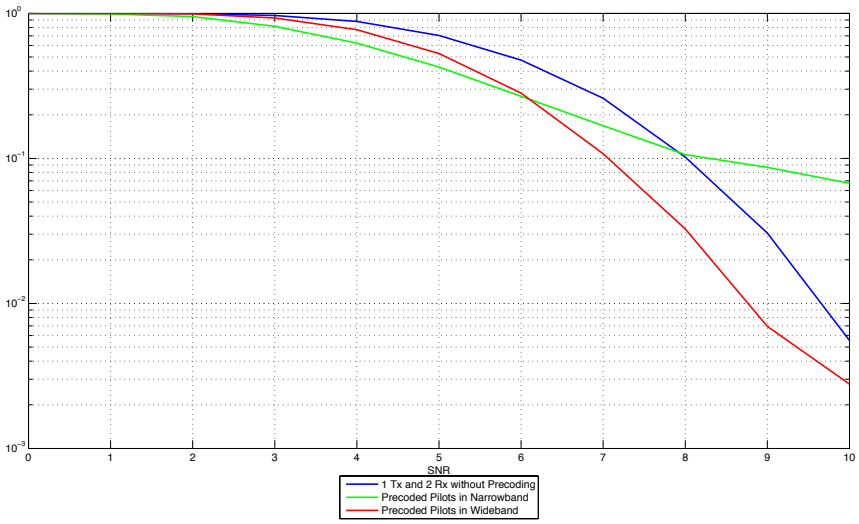

Figure 5.6: Block Error Rate of Precoded Pilots - Wideband vs Narrowband

The fact that the spectral efficiency of NB precoding do not reach the value of the reference system at a high value of SNR is confirmed since we consider the BLER graph. At a 10 % BLER threshold, NB precoding does not have a gain, but a loss of $0.292dB$ which is not acceptable. However, WB precoding has a gain of $0.927dB$ at a 10 % BLER threshold.

In addition to increase significantly the PAPR of symbols, NB precoding on pilots is disappointing with its performance.

Concerning WB precoding, its performance is not so efficient. It can be explained by the exceptions of the section 4.6.5, a WB precoding leads inevitably to a loss of resolution when it is applied over the whole transmission bandwidth.

Influence of the Calibration Error

To have a more realistic approach, we consider that the channel reciprocity, as it is defined in the section 3.1.1, is not perfect. So, according to the mathematical description given in the section 4.6.4, a calibration error between transmitter and receiver is considered.

Since NB precoding cannot be used, we chose to compare the impact of calibration error on WB precoding.

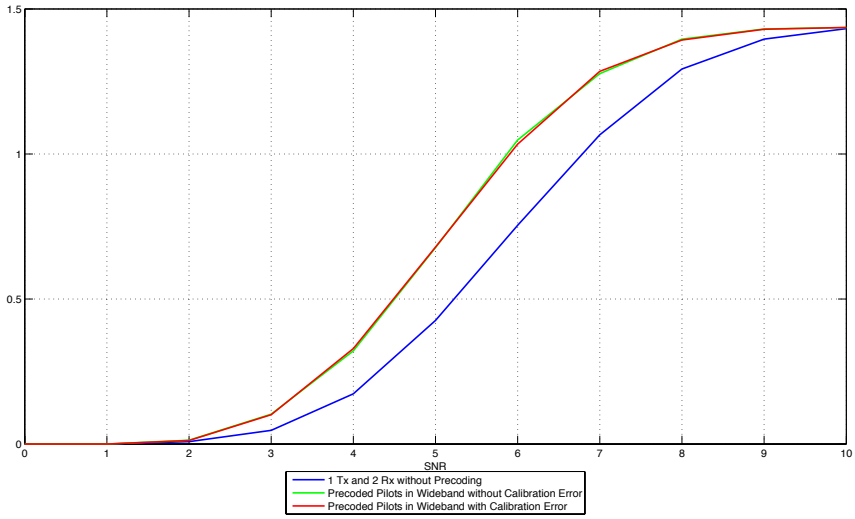

Figure 5.7: Comparison of influence of the Calibration Error

The maximal gain between WB precoding without calibration error and WB precoding with calibration error is up to $0.014dB$. This difference of gain between these two curves confirmed the exceptions made in the section 4.6.4, the calibration error has a very small influence on precoding performances.

Moreover, the gain at a 10 % BLER threshold has also been measured. According to the previous low value, here we have a gain of $0.058dB$ if the calibration error is not activated which also negligible.

2x4 Configurations

As we mentioned earlier, a system composed of two transmit antennas and four receiver antennas is one of the scenario assumed by 3GPP.

Here, we quantity the amount of gain provides by a WB and a NB precoding. It also gives the opportunity to confirm the results of the section 5.2.2 since only the number of receiver has increased.

The reference has been, of course, adapted in order to provide a relevant quantification of the amount of gain earned. We chose a SIMO system with four receive antennas as the section 4.2.2 defines it.

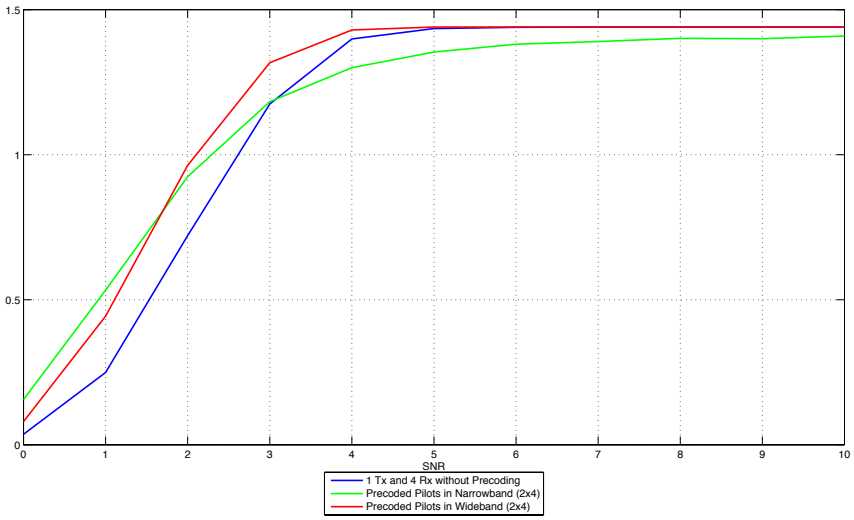

Figure 5.8: Spectral Efficiency of Precoded Pilots (2x4) - Wideband vs Narrowband

The figure 5.8, which shows the spectral efficiency, permits to determine that the maximum gain provides by the NB precoding is up to $0.284dB$. In the same time, WB precoding provides a maximal gain up to $0.182dB$.

The shape of these curves clearly remind the figure 5.5, the NB precoding gives worst performances than the SIMO reference system after a certain SNR. However, we now able to see that the NB precoding will reach the maximal value but at a very high SNR compared to WB precoding or to the SIMO system.

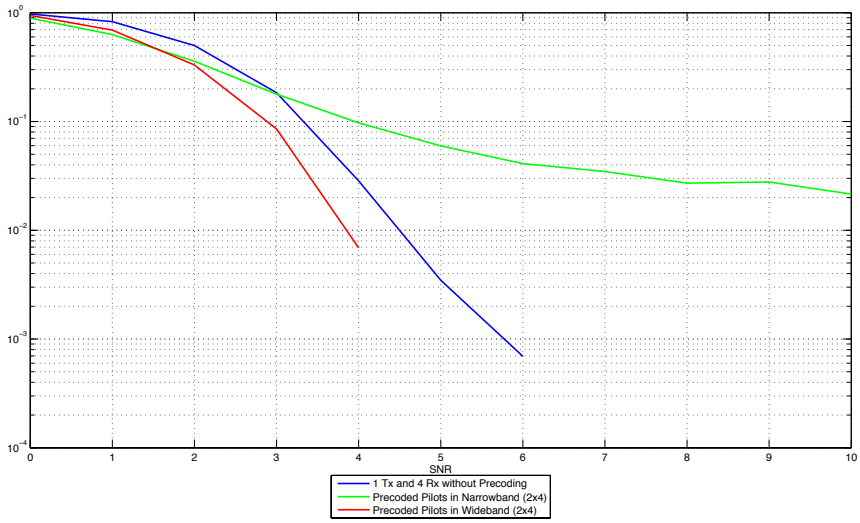

Figure 5.9: Block Error Rate of Precoded Pilots (2x4) - Wideband vs Narrowband

The fact that the spectral efficiency of NB precoding do not reach the value of the reference system at a high value of SNR is confirmed since we consider the BLER graph. At a 10 % BLER threshold, NB precoding does not have a gain, but a loss of $0.425dB$ which is not acceptable. However, WB precoding has a gain of $0.600dB$ at a 10 % BLER threshold.

Remarks for these results are exactly the same than in the section 5.2.2 but we can noticed that the amount of gain earned with WB precoding is more thin than WB precoding in a 2-by-2 system. So, a comparison between these curves is needed.

2x2 vs 2x4 Configurations

In order to evaluate the influence of the number of receive antennas, it is necessary to compare WB precoding curves. Each of these curves is compared with its own reference.

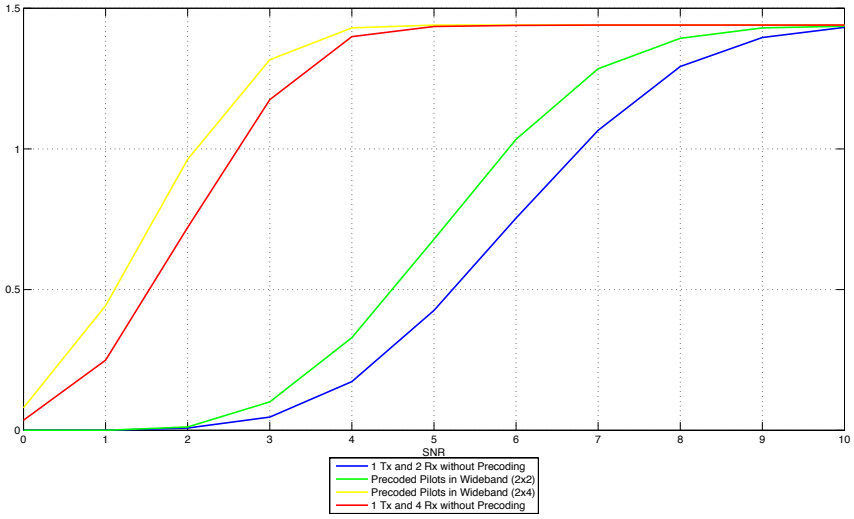

Figure 5.10: Spectral Efficiency of Precoded Pilots - 2x2 vs 2x4 Configurations (in WB)

The spectral efficiency gives a maximal gain up to $1.226dB$ if we compared both reference systems. And only $1.128dB$ if we compared both WB precoding curves.

As figures suggested it, the amount of gain earned by using precoding becomes more thin if the number of receive antennas increase.

In order to give an idea of this "shrinkage", we can define a ratio as follows:

$$E_{prec} = \frac{G_{prec}}{G_{ref}}$$

where G_{prec} is the amount of gain earned by adding receive antennas with WB precoding and G_{ref} is the amount of gain earned by adding receive antennas to SIMO systems.

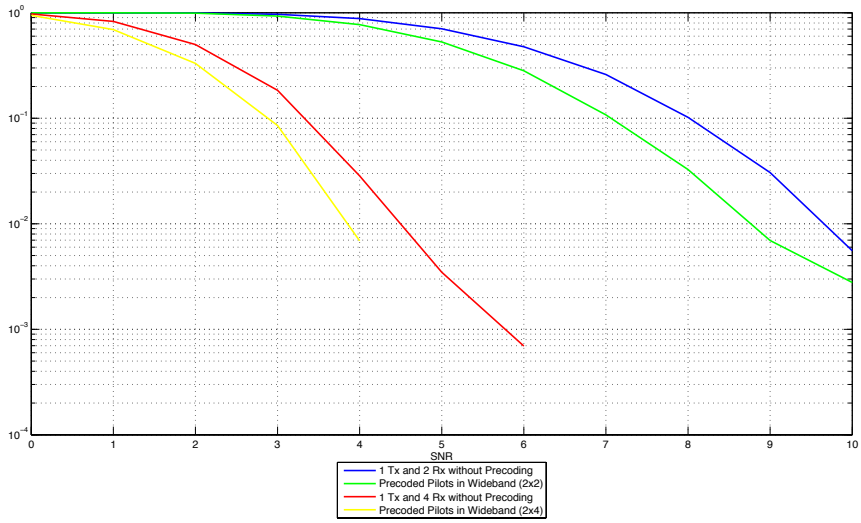

Figure 5.11: Block Error Rate of Precoded Pilots - 2x2 vs 2x4 Configurations (in WB)

At a 10 % BLER threshold, we have $G_{prec} = 4.074dB$ and $G_{ref} = 4.753dB$. So, since the gain is measured at the same value contrary to the spectral efficiency where we measured a maximal gain, we can define "the shrinkage of precoding" as:

$$1 - E_{prec} = 0.143$$

So, we can conclude that WB precoding in a 2-by-4 system is 14.3% less efficient than is a 2-by-2 system.

5.2.3 Phase based Precoding

The phase based precoding technique is defined as a phase precoding of pilots instead of precoding its amplitude and phase. So, it is to understand that performances are excepted to be lower than the precoded pilots technique defied previously.

Wideband vs Narrowband

As always, we make a comparison between NB precoding and WB precoding.

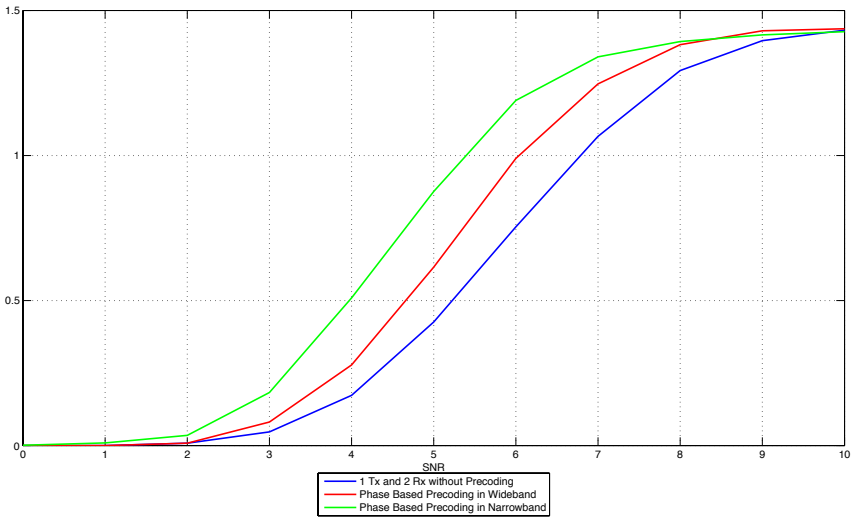

Figure 5.12: Spectral Efficiency of a Phase Based Precoding - Wideband vs Narrowband

Surprisingly, the amount of maximal gain provides by the Spectral Efficiency graph is up to $0.450dB$ by sung NB precoding and up to $0.236bB$.

If conclusions on these are the same than previously. We can be surprise by the thin quantity of gain losses by precoding only the phase.

At a 10 % BLER, we measured a gain of $0.666dB$ between the WB precoding and the reference system and surprisingly a gain of $1.322dB$ between the NB precoding and the reference system.

Actually, since the amplitude is not precoded any more, channel statistics are not forced

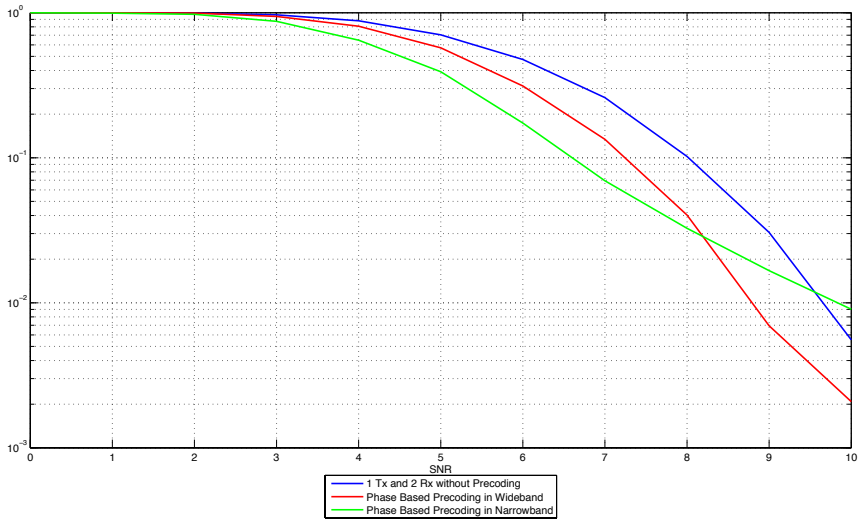

Figure 5.13: Block Error Rate of a Phase Based Precoding - Wideband vs Narrowband

as with a precoding in amplitude and phase. That is why it seems that NB precoding gives better results. However, the high PAPR provides by this precoding, as the figure 4.9 shows it, does not allow us to consider NB precoding as a solution.

Power Allocation of Antennas

We defined the phase based precoding technique as an evolution of precoded pilots technique in the section 3.4. The aim of this solution is to provide a equal power allocation for each transmitted subframes in order to simplify the implementation of the power amplifier.

As we can see on the figure 5.14, the power allocation with the precoded pilots technique gives a widely distribution of power allocation. It is this phenomenon that we wanted to avoid.

However, the power allocation with a precoding based only on the phase permit to have an equal power allocation between each transmitted subframes. As we excepted, this precoding provides a power balance.

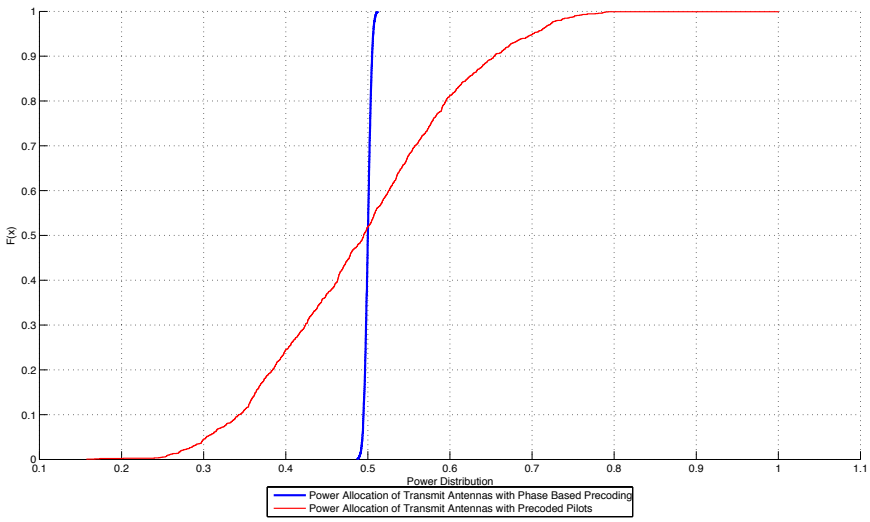

Figure 5.14: CDF of the Power Allocation of Transmit Antennas

5.2.4 Final Comparison

In order to quantify each suitable solution, meaning WB precoding with precoded pilots technique and phase based precoding technique, we chose to compare each with a closed-loop transmission with an unquantified feedback in NB, as it is defined in the section 2.4.

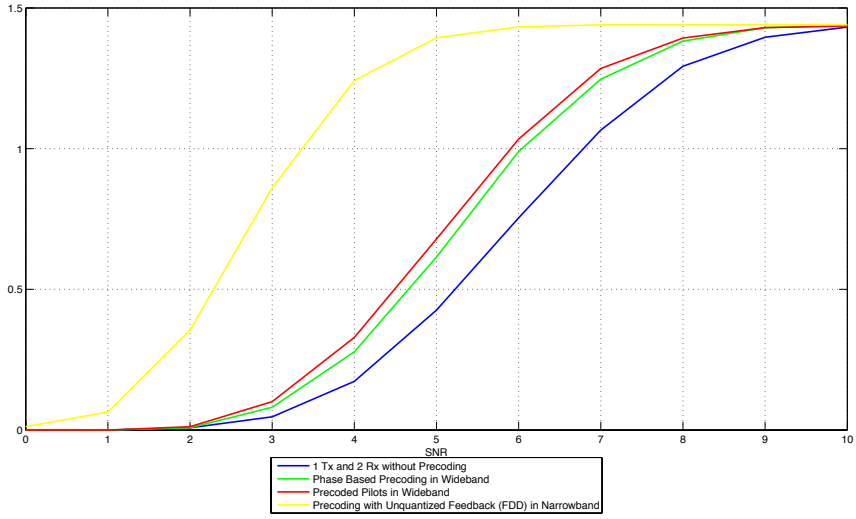

Figure 5.15: Spectral Efficiency of each precoding technique

Here, it becomes obvious that precoding solutions in open-loop transmission do not have high performances compared to a NB precoding in closed-loop transmission with an unquantified feedback. We measured a maximal gain up to $1.069dB$ when we compare the precoding in closed loop with the SIMO reference system. It is almost five times more than open-loop transmission which a maximal gain up to $0.280dB$ and $0.236dB$ for WB precoding with precoded pilots technique and phase based precoding technique, respectively.

It is also relevant to note that both curves in open-loop transmission are very close from each other which confirmed the reduced loss of performances if we precode only the phase of pilots.

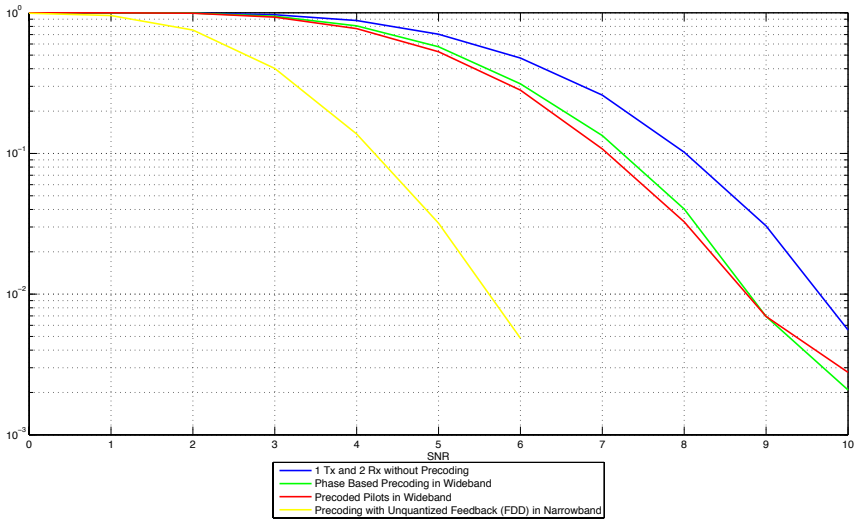

Figure 5.16: Block Error Rate of each precoding technique

At 10 % BLER, it becomes even more obvious that NB precoding with unquantified feedback, precoding is much more efficient than precoding on pilots. We measured a gain of $3.674dB$ for the precoding in closed-loop instead of $0.927dB$ and $0.666dB$ for open-loop transmission with precoded pilots technique and phase based precoding technique, respectively.

However, this comparison is not very fair since WB precoding are considered in opened-loop. The figure 5.17 shows a comparison of each WB precoding.

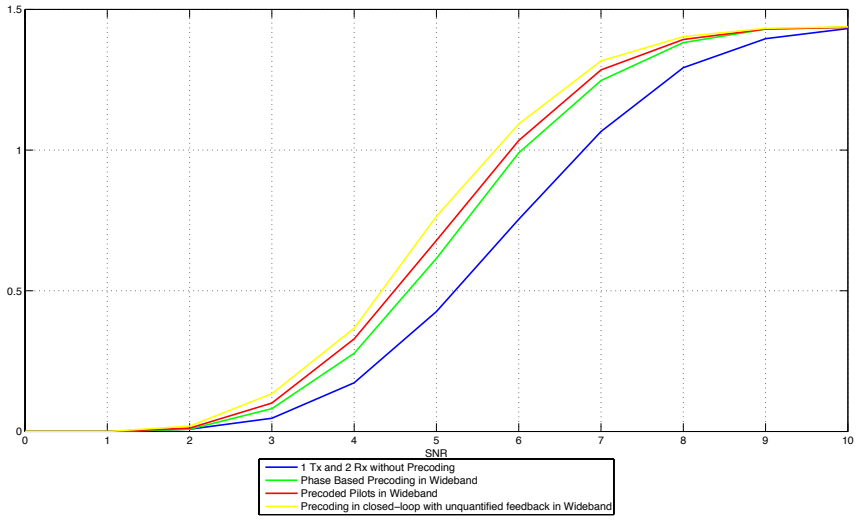

Figure 5.17: Spectral Efficiency of each WB precoding technique

Here, we measured a gain maximal up to $0.368dB$ when we do a comparison between the WB precoding in closed-loop transmission with unquantified feedback and the SIMO reference system.

So, when WB precoding is considered performance of precoding are closed to each other. Even, if WB precoding in open-loop cannot reach the same values than WB precoding with unquantified feedback.

Chapter 6

Conclusions

6.1 Interpretations of the results

According to comments made in the previous chapter, applying a precoding on a TDD mode transmission gives only a limited improvement of performances. Moreover, precoding in NB has to be excluded since it increased the PAPR of the symbols. To have a better overview of results, the figure 6.1 resumes all the gains that precoding techniques provide compared to a SIMO system without precoding in a 2x2 system.

Precoding Technique	Size of Precoding	Maximal Gain (Spectral Efficiency)	Gain (BLER)
Blind Precoding	Narrowband	0.068	NaN
	Wideband	NaN	NaN
Precoded Pilots	Narrowband	0.400	-0.292
	Wideband	0.280	0.927
Phase based Precoding	Narrowband	0.450	1.322
	Wideband	0.236	0.666
Precoding with Unquantized Feedback	Narrowband	1.069	3.6738
	Wideband	0.368	1.254

Figure 6.1: Comparison between gains provide by each precoding techniques

Here, it becomes obvious that the unquantified feedback in a closed-loop transmission extremely improves performances if a precoding in NB is applied but it cannot be considered

as a realistic solution. That is why we cannot expect that results in TDD mode surpass this model of transmission but we can consider that it represents the upper edge as a reference, like SIMO system represents the lower edge.

However, WB precoding gives almost same improvements of performance in closed-loop and open-loop transmission even if benefits are limited compared to a SIMO system. WB precoding in open-loop only has thin losses compared to WB precoding in closed-loop.

Note also that when the precoding on pilots is only based on the phase, only a thin loss has been noticed compared to pilots precoding in amplitude and phase. Moreover, we earned a almost balanced power of transmit antenna between each subframes compared to precoded pilots technique.

Since, we also considered precoding with a 2x4 system, the figure 6.2 resumes the gain of precoded pilots technique in this system:

Precoding Technique	Size of Precoding	Maximal Gain (Spectral Efficiency)	Gain (BLER)
Precoded Pilots (2x4)	Narrowband	0.284	-0.425
	Wideband	0.242	0.600

Figure 6.2: Comparison between gains provide precoded pilots technique in a 2x4 system

To conclude, we can say that WB precoded pilots transmission in TDD are disappointing because their performance gives only a limited benefits compared to a SIMO system without precoding. If the aim of precoding is to improve significantly transmission performances, it is not so relevant when WB precoding on pilots is considered and it is even worst when blind transmission is used since only losses have been evaluated when a realistic time delay between frames is assumed.

6.2 Future Work

As we saw, the evaluation of precoded pilots transmission in TDD mode does not perform a relevant improvement of performances compared to a SIMO system without precoding. So, in order to have significant results, it is necessary to investigate other precoding solutions but based on a different concept.

However, there are several ways to continue the investigation of this current precoding. If the configuration 2x2 and 2x4 were also one of 3GPP assumptions [24] for its self-evaluation, the uplink channel in LTE-Advanced allows a number of transmit antennas up to four. In this way, different number of multi-streams transmission has to be considered and evaluated. It could be a relevant modelling since only a single stream transmission is considered in this report.

Moreover one of main assumptions was considering SU-MIMO, it is possible to evaluate the impact precoded transmission in TDD mode on MU-MIMO with different algorithms of resources allocation currently being developed [8].

Bibliography

[1] 3GAmericas. *3GPP Mobile Broadband Innovation Path to 4G, Release 9, Release 10 and Beyond, HSPA+, LTE/SAE and LTE-Advanced*. February 2010.

[2] 3GPP. Ts 34.121 v6.0.0 - technical specification group terminals - terminal conformance specification - radio transmission and reception (fdd). Technical report, 2006.

[3] 3GPP. 3gpp tr 36.913 - technical specification group radio access network, requirements for further advancements. Technical report, December 2009.

[4] 3GPP. R1-090943 : Non-codebook-based precoding for uplink transmission. Technical report, February 2009.

[5] 3GPP. 3gpp tr 36.211 - technical specification group radio access network - evolved universal terrestrial radio access (e-utra) - physical channels and modulation (release 8). Technical report, March 2009.

[6] 3G Americas. 3gpp lte for tdd spectrum in the americas. November 2009.

[7] J. Uhl B. Davis. *Matrices, Geometry and Mathematica*. Math Everywhere, Inc, 1999.

[8] B.Trouilleux B. Thomas, A. Truchon. Multi-carrier distributed system for local area indoor hotspot. This report is not yet validated but it will be soon.

[9] Takehiro Nakamura 3GPP TSG-RAN Chairman. Proposal for candidate radio interface technologies for imt-advanced based on lte release 10 and beyond. 15 October 2009.

[10] Takehiro Nakamura 3GPP TSG-RAN Chairman. Lte-advanced (3gpp release 10 and beyond) - rf aspects. December 2009.

[11] Peter Skov-Wang Haiming Che Xiangguang, Troels Kolding and Antti Toskala. *LTE TDD Mode*. 2009.

[12] Josep Colom Ikuno Dagmar Bosanska Markus Rupp Christian Mehlfuhrer, Martin Wrulich. Simulating the long term evolution physical layer. August 2009.

[13] Ylva Jading Magnus Lindstrom Erik Dahlman, Anders Furuskaar and Stefan Parkvall. Key features of the lte radio interface. *Ericsson Review No. 2*, pages 77–80, 2008.

[14] P.Mogensen K.Pajukoski G.Berardinelli, T.B.Sorensen. Precoded multirank transmission with linear receivers for lte-a uplink. *Proc. of IEEE 70th Vehicular Technology Conference*, September 2009.

[15] Simone Frattasi Troels B.Sorensen Preben Mogensen Kari Pajukoski Gilberto Berardinelli, Luis Angel Maestro Ruiz de Temino. On the feasibility of precoded single user mimo for lte-a uplink. April 2009.

[16] Alexandre Vanaev Holger Busche and Hermann Rohling. Svd based mimo precoding and equalization schemes for realistic channel estimation procedures. In *Frequenz 61*.

[17] Jin-Kyu Han Juho Lee and Jianzhong Zhang. Mimo technologies in 3gpp lte and lte-advanced. *EURASIP Journal on Wireless Communications and Networking*, 2009.

[18] Meik Kottkamp. Lte-advanced technology introduction. Technical report, February 2009.

[19] Huseyin Arslan Mehmet Kemal Ozdemir and Ercument Arvas. Mimo-ofdm channel estimation for correlated fading channels.

[20] MIET Moray Rumney BSc, C. Eng. 3gpp lte: Introducing single-carrier fdma. 2009.

[21] Telecommunication Engineering Centre (TEC) Ministry of Communications and Government of India Information Technology. Study paper on scalable ofdma. June 2007.

[22] Basuki Endah Priyanto. *Air Interfaces of Beyond 3G systems with User Equipment Hardware Imperfections: Performance and Requirements Aspects*. PhD thesis, Aalborg University, February 2008.

[23] Christoph Windpassinger Robert F.H. Fischer, Clemens Stierstorfer. Precoding and signal shaping for transmission over mimo channels. 2009.

[24] Tetsushi Abe (NTT DOCOMO 3GPP TSG-RAN1 Vice-Chairman). 3gpp self-evaluation methodology and results - assumptions. Technical report, 2009.

[25] Ernesto Zimmermann-Peter Zillmann-Denis Petrovic Marcus Windisch Olivier Seller Pierre Siohan Merouane Debbah David Gesbert Gros Roger Sophia Antipolis Kari Kalliojarvi Liesbet van der Perre Volker Jungnickel, Eduard Jorswiek. Mimo-ofdm in the tdd mode. 2009.

[26] Jong-Gwan Yook Woo-Ghee Chung, Euntaek Lim and Han-Kyu Park. Calculation of spectral efficiency for estimating spectrum requirements of imt-advanced in korean mobile communication environments. pages 153–161, April 2007.